Equations of state and thermodynamics of solids using empirical corrections in the quasiharmonic approximation

A. Otero-de-la-Roza* and Víctor Luaña†

Departamento de Química Física y Analítica, Facultad de Química, Universidad de Oviedo, ES-33006 Oviedo, Spain

(Received 24 May 2011; revised manuscript received 8 October 2011; published 11 November 2011)

Current state-of-the-art thermodynamic calculations using approximate density functionals in the quasiharmonic approximation (QHA) suffer from systematic errors in the prediction of the equation of state and thermodynamic properties of a solid. In this paper, we propose three simple and theoretically sound empirical corrections to the static energy that use one, or at most two, easily accessible experimental parameters: the room-temperature volume and bulk modulus. Coupled with an appropriate numerical fitting technique, we show that experimental results for three model systems (MgO, fcc Al, and diamond) can be reproduced to a very high accuracy in wide ranges of pressure and temperature. In the best available combination of functional and empirical correction, the predictive power of the DFT + QHA approach is restored. The calculation of the volume-dependent phonon density of states required by QHA can be too expensive, and we have explored simplified thermal models in several phases of Fe. The empirical correction works as expected, but the approximate nature of the simplified thermal model limits significantly the range of validity of the results.

DOI: 10.1103/PhysRevB.84.184103 PACS number(s): 64.10.+h, 65.40.−b, 63.20.−e, 71.15.Nc

I. INTRODUCTION

The reliable and inexpensive determination of equations of state (EOS), thermodynamic properties, and phase stability of solids is one of the fundamental problems in condensed matter physics, materials science, and geophysics. The first-principles method of reference for the calculation of such objects is the density functional theory[1,2] (DFT), the main component (the exchange-correlation functional) of which is unknown. On top of DFT, in order to access the properties of a solid at relatively low temperatures, the approach commonly employed consists of assuming a harmonic potential for the atoms at any crystal structure: the quasiharmonic approximation (QHA).[3,4] In this paper, we show how the systematic errors induced by the approximate exchange-correlation functional at the DFT level preclude accurate thermodynamic calculations in the framework of QHA (Refs. 5–7) and how simple empirical corrections of the static energy improve the theoretical predictions to experimental accuracy.

The suitability of different approximate exchange-correlation functionals for the calculation of thermodynamic properties and other tasks has been examined in a long list of articles benchmarking their performance (for instance, see Refs. 6 and 8–12,), mainly in terms of the equilibrium volumes, bulk moduli, and cohesion energies of simple solids. From these works, clear trends are apparent: local density approximation (LDA) tends to overbind, that is, it yields equilibrium volumes too small and equilibrium bulk moduli too large compared to experimental results, and generalized gradient approximation (GGA) functionals tend to the opposite effect. Unfortunately, current state-of-the-art DFT calculations are unable to predict, without further experimental confirmation, the p-V-T equation of state, let alone more complex thermodynamic properties of a solid.[5,7] Although LDA and GGA functionals usually bracket the correct volume and bulk modulus,[5,12] not even this well-known behavior holds for every crystal.[7,11]

There have been insights in the literature about how these systematic deviations can be corrected. For instance, van de Walle and Ceder[13] noted that LDA bulk moduli and elastic properties computed at the experimental geometry compare better with experimental results than those obtained at the equilibrium geometry. Kunc and Syassen[14] showed that p/B_0 versus V/V_0 curves are transferable, nearly independent of the functional, and close to their experimental counterpart (V_0 and B_0 being the static equilibrium volume and bulk modulus). Grabowski *et al.*[12] performed a careful benchmark of LDA and GGA in the computation of thermodynamic properties of elemental nonmagnetic face-centered-cubic (fcc) metals and reached the conclusion that LDA and Perdew-Burke-Ernzerhof (PBE) functionals bracket the correct experimental results, and that LDA performs better than PBE in the computation of heat capacities and thermal expansivities. In addition, it is well known that phonon densities of states as well as other properties related to derivatives of the static energy agree better with experimental observations if calculated at the experimental volume, but only at the GGA level,[5,6,15–19] and that the agreement of LDA, PBE, and experimental results is better for cell shapes and atomic positions than for volumes themselves.[6] The GGA and LDA phonon density of states are, for nonmagnetic materials, a scaled version of each other with minor differences (for magnetic materials, however, the comparison is not so simple[7]).

Because the correct functional is unknown, and given the difficulty in climbing the metaphoric "Jacob's ladder,"[20] we propose a method that uses a few experimental data to correct the observed systematic deviations: using empirical energy corrections[21] (EEC). The EEC are expressions that replace the static energy, thus modifying the pressure and temperature-dependent equilibrium volumes, but not the vibrational properties associated to each volume. The corrections require a thermal model to introduce the information contained in the experimental parameters. We use the complete version of the QHA: on a fixed grid of volumes, the phonon density of states $g(\omega; V)$ are calculated at the relaxed geometry. The $g(\omega; V)$ are associated to volumes, and are independent of how

the static energy and its derivatives are corrected. We examine three EECs in Sec. II.

To test the performance of the EECs, we have carried out QHA calculations on three simple solids with different bonding patterns, MgO ($B1$ phase), fcc Al, and diamond, using plane-wave basis sets and ultrasoft pseudopotentials in the framework of the density functional perturbation theory[22] (DFPT) with LDA and GGA functionals. We have chosen these systems not only because of their simplicity and popularity, which warrants the abundance of experimental data to compare with, but also because of their cubic symmetry: volumetric temperature effects manifest through a diagonal thermal stress (that is, a thermal pressure), simplifying the analysis of the error sources in the corrections.[23] This does not imply, however, that the EECs are limited to cubic systems. The correction can be used on crystals of arbitrary shape and complexity. An account of the calculation details is given in Sec. III.

A fundamental property of materials is the pressure-volume-temperature equation of state $V(p,T)$. In Sec. IV, we analyze how the application of EECs allows us to predict $V(p,T)$ with accuracy comparable to experiment and with independence of the functional, provided the (functional-dependent) limit of validity of QHA is not exceeded. The six functional plus EEC combinations examined are compared and we observe that the temperature range of validity of the LDA equation of state is more restricted than PBE due to the earlier onset of the intrinsic anharmonic regime. Using the best EEC and functional choice found, we propose a $V(p,T)$ expression fitted to our *ab initio* results on a pressure-temperature grid spanning a wide range of conditions for the three systems under study.

The application of EECs also influences other thermodynamic properties. In Sec. V, we analyze these effects on a collection of properties at ambient conditions, and on the adiabatic bulk modulus, heat capacity, and thermal expansivity on a range of pressures and temperatures. The Gibbs free energy plays an essential role in phase stability and the computation of phase diagrams, so the impact of the static energy correction on G is carefully examined. The analysis shows that the use of EEC improves the consistency of the calculations and the agreement with experiment, and insight regarding the relative performance of LDA and PBE functionals can be extracted.

Finally, in Sec. VI, we present an application of the new techniques in a more complex material: body-centered-cubic (bcc) iron. We show how the use of EECs is simplified by approximate thermal models and generalize the correction equations to arbitrary pressures and temperatures. The results for iron also hint that, for magnetic materials, the EECs only correct part of the discrepancies. The approximate models allow applying EECs with a cost comparable to that of calculating the static energy curve, but the results are not as good as using the full QHA.

II. DEFINITION OF THE EMPIRICAL ENERGY CORRECTIONS

In a previous paper,[21] we proposed a systematic procedure to obtain the EOS of magnesium oxide from raw QHA data with accuracy comparable to experiment. This method is based on (i) the use of averages of strain polynomials to robustly represent the $E(V)$ function and its derivatives and (ii) an empirical correction of the static energy. Part one of the procedure has been thoroughly explored in previous papers,[24,25] while it is the second part of the procedure with which we are mainly concerned in this paper.

Several authors have tackled the problem of the systematic errors in DFT volumes and elastic properties in different ways. The simplest method is using a *magic bullet*: exploring the available functionals and turning the knobs of the calculation (pseudopotentials, basis set, . . .) until a satisfactory agreement with experimental data is obtained. Of course, this method is computationally awkward, theoretically doubtful, and not systematic. Another option is selecting a good-quality experimental data set and fitting the *ab initio* results to it by using some functional form, with the purpose of extrapolating to regions unexplored by experiment. This is, for instance, the approach used by Wu *et al.*[26,27] to calculate the equation of state of MgO. In their work, they correct the raw $V(p)$ curve with an additive term

$$\Delta V = \Delta V_0 \exp(-p/p_c), \tag{1}$$

where ΔV_0 and p_c are parameters chosen to fit an experimental equation of state. Generalizing this method is problematic: the correcting expression is *ad hoc*, requires a good experimental data set, which limits the applicability of the method to very-well-studied solids, and presents the uncertainties typical of a fitting procedure.

Another popular approach is applying a constant pressure shift[12,13] in a manner similar to the PSHIFT correction proposed below. In this paper, we enhance this simple scheme by (i) taking into full account the thermal effects on the solid and (ii) proposing more involved corrections that improve upon the simple pV shift.

In this section, we present practical procedures to scale the *ab initio* $E(V) = E_{\rm sta}(V)$ data for the calculation of thermodynamic properties by using an empirical approach involving one or at most two accurate and easily accessible experimental parameters. These data are the experimental volume and bulk modulus at ambient conditions, henceforth labeled $V^0_{\rm expt}$ and $B^0_{\rm expt}$ (the room temperature is $T^0 = 298.15$ K). The EEC coefficients are calculated using the uncorrected data, which we refer to using the subscript "sta" (for static). For future reference, the static uncorrected equilibrium volume and bulk modulus are labeled V_0 and B_0, respectively.

The starting point is the nonequilibrium or generalized Gibbs free energy

$$G^*(\boldsymbol{x},V;p,T) = E_{\rm sta}(\boldsymbol{x},V) + pV + F^*_{\rm vib}(\boldsymbol{x},V;T), \tag{2}$$

where $E_{\rm sta}$ is the static energy and $F^*_{\rm vib}$ is the nonequilibrium vibrational Helmholtz free energy. The cell volume V together with the rest of free-cell coordinates $\boldsymbol{x}$ determine completely the geometry of the crystal. For a given pressure and temperature, the equilibrium configuration is given by the $\boldsymbol{x}$ and V that minimize G^*. The value of G^* at that minimum is the equilibrium Gibbs free energy $G(p,T)$. If, for a fixed volume,

the internal coordinates are relaxed, $\boldsymbol{x}(p,T)$ is obtained by minimization of Eq. (2), resulting in

$$G^*(V;p,T) = \min_{\boldsymbol{x}} G^*(\boldsymbol{x},V;p,T) = E_{\rm sta}(V) + pV + F^*_{\rm vib}(V,T). \quad (3)$$

As our test systems do not present degrees of freedom related to the atomic positions or the cell shape, we use the latter expression. The same EEC expressions apply straightforwardly to arbitrary symmetry solids.

In the quasiharmonic approximation, the nonequilibrium vibrational Helmholtz free energy is

$$F^*_{\rm vib}(\boldsymbol{x},V;T) = \int_0^\infty \left[\frac{\omega}{2} + k_B T \ln(1 - e^{-\omega/k_B T})\right] \times g(\omega;\boldsymbol{x},V)d\omega. \quad (4)$$

In a similar way, the equilibrium vibrational Helmholtz free energy is given by $F(V,T) = F^*_{\rm vib}[V(p,T);T]$, where $V(p,T)$ is the equilibrium volume at the given conditions.

If the static energy is replaced by a corrected energy $\tilde{E}_{\rm sta}(V)$, the resulting modified static pressure $\tilde{p}_{\rm sta} = -d\tilde{E}_{\rm sta}/dV$ affects the equilibrium volumes through the equilibrium condition

$$-\frac{\partial \tilde{G}^*}{\partial V}(V;p,T) = 0 = \tilde{p}_{\rm sta} - p + p_{\rm th}, \quad (5)$$

but the phonon density of states (phDOS) at a given volume $F^*_{\rm vib}$ and the thermal pressure $p_{\rm th} = -\partial F^*_{\rm vib}/\partial V$ are not affected. This is important because phDOS are affected to a lesser extent by systematic errors at DFT level than equilibrium volumes.

We examine three different empirical energy correction methods:

(1) The PSHIFT correction shifts the energy by a constant pressure Δp:

$$\tilde{E}_{\rm sta}(V) = E_{\rm sta}(V) + \Delta p V. \quad (6)$$

This approach is by far the most popular[12,28] and has been given theoretical justification by van de Walle and Ceder[13] as a modification of the LDA functional. The correction shifts the static equilibrium volume by adding Δp to the equilibrium equation (5), without affecting the bulk modulus or higher derivatives of the energy. In their work, van de Walle and Ceder proposed calculating Δp as a weighted average of atomic pressures, obtained in turn in some elemental phase. In contrast, we use the experimental datum $V^0_{\rm expt}$ to find the Δp, which gives

$$-\frac{\partial \tilde{G}^*}{\partial V}\left(V^0_{\rm expt};0,T^0\right) = 0. \quad (7)$$

Solving this equation leads to

$$\Delta p = p(V_{\rm expt},T^0) = p_{\rm sta}\left(V^0_{\rm expt}\right) + p_{\rm th}\left(V^0_{\rm expt},T^0\right). \quad (8)$$

The value of the Δp parameter is calculated using the uncorrected data alone, and the resulting static energy yields a T^0 and 0 GPa equilibrium volume exactly equal to the experimental datum $V^0_{\rm expt}$. In a naïve implementation of this correction, the thermal model would be missing and the static volume would be fit to the experimental volume by neglecting $p_{\rm th}$. This is a fundamental error because the thermal pressure is of the same order as the static pressures (and possibly larger!).

(2) In the same style, we can develop an EEC based on the correction proposed by Alchagirov *et al.*,[28] which we call APBAF, after the initials of the authors. In that and subsequent works,[8] it recognized the need of a correction for the description of the core-valence interaction in DFT calculations. The authors argue that such error is contained in a term of the form V^{-1}, so the corresponding EEC can be formulated as

$$\tilde{E}_{\rm sta}(V) = E_{\rm sta}(V) + \frac{\alpha}{V}. \quad (9)$$

Using a procedure similar to the previous EEC, we obtain the value of α that exactly fits the experimental $V^0_{\rm expt}$ value:

$$\alpha = -p\left(V^0_{\rm expt},T^0\right)\left(V^0_{\rm expt}\right)^2. \quad (10)$$

(3) The last EEC we propose (called BPSCAL) uses two experimental data: $V^0_{\rm expt}$ and $B^0_{\rm expt}$. This correction is inspired on the observation by Kunc and Syassen[14] that static p/B_0 versus V/V_0 curves closely match for LDA and GGA functionals, and also for the experimental curve. In terms of a correction of the static energy, this translates into finding a $\tilde{E}_{\rm sta}$ such that

$$\frac{\tilde{E}'_{\rm sta}(V)}{B_{\rm expt}} = \frac{E'_{\rm sta}\left(V\frac{V_0}{V_{\rm expt}}\right)}{B_0}, \quad (11)$$

where the primes indicate volume derivatives and $V_{\rm expt}$ and $B_{\rm expt}$ are the experimental static volume and bulk modulus extrapolated to static conditions (cf. the experimental room-temperature equivalents $V^0_{\rm expt}$ and $B^0_{\rm expt}$). Integrating the above equation leads to the expression of the EEC

$$\tilde{E}_{\rm sta}(V) = E_{\rm sta}(V_0) + \frac{B_{\rm expt}V_{\rm expt}}{B_0 V_0}\left[E_{\rm sta}\left(V\frac{V_0}{V_{\rm expt}}\right) - E_{\rm sta}(V_0)\right]. \quad (12)$$

The arbitrary integration constant $\tilde{E}_{\rm sta}(V_{\rm expt})$ is made equal to $E_{\rm sta}(V_0)$ so that the correction vanishes in the limit $V_{\rm expt} = V_0$ and $B_{\rm expt} = B_0$, thus keeping the energy footing of the original data. This is useful in case the correction is used in the context of the determination of phase equilibria. The energy derivatives of the corrected energy are

$$\tilde{E}'_{\rm sta}(V) = \frac{B_{\rm expt}}{B_0}E'_{\rm sta}\left(V\frac{V_0}{V_{\rm expt}}\right), \quad (13)$$

$$\tilde{E}''_{\rm sta}(V) = \frac{B_{\rm expt}V_0}{B_0 V_{\rm expt}}E''_{\rm sta}\left(V\frac{V_0}{V_{\rm expt}}\right), \quad (14)$$

so the condition given by Eq. (11) is met. In addition, $V_{\rm expt}$ is the corrected static equilibrium volume [$\tilde{E}'_{\rm sta}(V_{\rm expt}) = E'_{\rm sta}(V_0) = 0$] and $B_{\rm expt} = V_{\rm expt}E''_{\rm sta}(V_{\rm expt})$ is the corrected static equilibrium bulk modulus. The cohesion energy is modified according to

$$\tilde{E}_{\rm coh} = \frac{B_{\rm expt}V_{\rm expt}}{B_0 V_0}E_{\rm coh}. \quad (15)$$

The missing piece of this EEC is the procedure to obtain the extrapolated static experimental data $V_{\rm expt}$ and $B_{\rm expt}$ from their

TABLE I. Calculation parameters for the examined cases: MgO, diamond, and fcc Al. The Vs column corresponds to the number of data points forming the volume grid, E_{cut} is the plane-wave cutoff energy (Ry). Following this column, the electronic meshes and vibrational meshes (Monkhorst-Pack) are shown. The last two columns correspond to the electron configuration used to generate the pseudopotentials and the number of core electrons they represent.

	Vs	E_{cut}	$\boldsymbol{k}$ point	$\boldsymbol{q}$ point	Elec. config.	Core
MgO	174	80	$4 \times 4 \times 4$	$8 \times 8 \times 8$	Mg:$1s^2 2s^2 2p^6 3s^1$	2
					O:$1s^2 2s^2 2p^5$	2
C	31	60	$6 \times 6 \times 6$	$6 \times 6 \times 6$	$1s^2 2s^2 2p^2$	2
Al	43	50	$16 \times 16 \times 16$	$6 \times 6 \times 6$	$1s^2 2s^2 2p^6 3s^2 3p^1$	10

room-temperature counterparts. Imposing the equilibrium condition at V^0_{expt} yields

$$B_{\text{expt}} = -B_0 \frac{p_{\text{th}}(fV_0, T^0)}{p_{\text{sta}}(fV_0)}, \tag{16}$$

where the volume factor f is

$$f = \frac{V^0_{\text{expt}}}{V_{\text{expt}}}, \tag{17}$$

which is greater than 1 except in the rare solids with negative thermal expansion from static conditions to 300 K. The corrected isothermal bulk modulus at T^0 must be B^0_{expt}, so

$$\begin{aligned} B^0_{\text{expt}} &= \left(V \frac{\partial^2 F^*}{\partial V^2}\right)\left(V^0_{\text{expt}}, T^0\right) \\ &= \frac{B_{\text{expt}}}{B_0} B_{\text{sta}}(fV_0) + B_T\left(V^0_{\text{expt}}, T^0\right) - B_{\text{sta}}\left(V^0_{\text{expt}}\right). \end{aligned} \tag{18}$$

Combining Eqs. (16) and (18),

$$\frac{B_{\text{sta}}(fV_0)}{p_{\text{sta}}(fV_0)} = -\frac{B^0_{\text{expt}} - B_T\left(V^0_{\text{expt}}, T^0\right) + B_{\text{sta}}\left(V^0_{\text{expt}}\right)}{p_{\text{th}}\left(V^0_{\text{expt}}, T^0\right)}. \tag{19}$$

The right-hand side of the last equation is readily calculated using the uncorrected energy. Given V^0_{expt} and B^0_{expt}, a search is performed in the $V > V_0$ region (if the right-hand side is negative) or the $V < V_0$ region (if positive) for a factor f such that $B_{\text{sta}}/p_{\text{sta}}$ fulfills Eq. (19). This factor yields the experimental static volume and bulk modulus using Eqs. (17) and (16). In this EEC, both the experimental volume and bulk modulus are exactly matched to within the numerical precision allowed by the volume derivatives.

The three EECs assume that a temperature model is available to calculate the equilibrium volume at ambient conditions from first-principles data, but we make no assumption regarding the details of this model. In the most straightforward implementation, used in this work, this model is the quasiharmonic approximation (QHA). However, in cases where the computation of phonon dispersion relations on a grid of volumes is unfeasible, simplified models[29,30] of QHA (Debye,[31] Debye-Grüneisen,[32] ...) can be used as well. In such cases, the correction also reflects the quality of the thermal model. A simple application of approximate thermal models to iron is presented in Sec. VI.

Nevertheless, the use of a thermal model is essential in order to capture the temperature and zero-point effects necessary for a sensible comparison to experimental room-temperature data.[12] Indeed, these effects convey a correction to equilibrium volume and bulk modulus of the order of the LDA and GGA deviations,[15] although smaller, so exchange-correlation functional benchmarks can be misinterpreted if they are not accounted for.

III. CALCULATION DETAILS

With the purpose of testing the performance of the energy corrections, we have calculated three systems with different bonding schemes: a typical ionic solid (MgO, $B1$ phase), a covalent solid (diamond), and a metal (fcc Al). All three systems are cubic, and their behavior is experimentally well known.

A sufficiently fine volume grid was chosen and the energy and phonon density of states (phDOS) were calculated at each of those volumes using a pseudopotentials plus plane-waves approach and the density functional perturbation theory[22] (DFPT), as implemented in the QUANTUM ESPRESSO package.[33] Ultrasoft pseudopotentials[34] were generated for all the atoms involved using the USPP program by Vanderbilt. The convergence of the calculation parameters was checked against the phDOS. The configurations and number of core electrons of the pseudopotentials, together with the final parameters used, are given in Table I.

We have chosen two widely used exchange-correlation functionals to check the performance of the EECs: LDA in the parametrization of Perdew and Zunger[35] and the Perdew-Burke-Erzenhof version of GGA.[36] Although the EECs apply equally well to any functional, we have selected those functionals not only because of their popularity, but also because they coarsely represent an error bar that usually brackets the correct experimental results.[11]

An important topic in the accurate treatment of thermodynamic data is the use of an adequate equation of state. Very recently,[24,25] we have shown that averages of strain polynomials up to a high degree provide the robust treatment of first-principles data for thermodynamic calculations: the derivatives of the energy are accurate and the method provides a statistical way of estimating the errors in the calculated properties. Consequently, we have used an average up to twelfth-order polynomials in the Eulerian strain, fitted using the procedures described in Ref. 24. The second version of the GIBBS program[29,30] and the ASTURFIT octave interface[24] were used to process the data. The experimental volumes and bulk moduli used in the corrections are shown in Table II.

In the case of Al, there is a contribution to the thermodynamic properties due to the conducting electrons. We

TABLE II. Experimental data used in the correction of the *ab initio* static results for the three systems under study.

	V^0_{expt} (bohr^3)	B^0_{expt} (GPa)	Ref.
MgO	126.03	161.3	37
Diamond	76.58	446	38
Al	111.84	72.7	39,40

have used the Sommerfeld model of free and independent electrons to include its electronic contributions to the free energy.[41] The results are roughly equivalent to those calculated using the finite-temperature DFT formalism,[42] as is expected for a typical free-electron-like metal such as Al, and their effect on the calculated thermodynamic properties (except for the high-temperature heat capacity) is negligible for the temperatures considered.

IV. CORRECTED EQUATIONS OF STATE

A. Comparison to experimental results

The effects of the empirical energy corrections on the *ab initio* static energy of MgO are shown in Fig. 1. The three EEC schemes correct the static energy in a similar but not identical way. The energy minimum is displaced to a smaller value in PBE and to a larger value in LDA, correcting the well-known behavior of these functionals. The corrected static equilibrium volume is within a range of 0.36 bohr^3 for the three EECs.

The effects on the curvature of $E(V)$ are more subtle. By definition, the PSHIFT correction does not modify the second and higher derivatives of $E(V)$ and, therefore, it amounts to a horizontal translation of the uncorrected graph. In contrast, APBAF modifies the static bulk modulus

$$\tilde{B}_{\text{sta}} = B_{\text{sta}} + \frac{\alpha}{2V^2}, \tag{20}$$

and for BPSCAL, the static equilibrium bulk modulus is made to be equal to the calculated B_{expt}, higher than B^0_{expt} because of the thermal and especially the zero-point effects. The resulting correction of the shape of $E(V)$ is similar for APBAF and BPSCAL: the solid is stiffer for LDA and softer for PBE. Surprisingly, the curvature correction is opposite to the effect on the volume. When the volume is corrected using the PSHIFT EEC, it is actually LDA that is underbinding and PBE that is overbinding with respect to the bulk modulus. This is consistent with previous observations in the literature[12] and is present in the LDA and PBE trends for all thermodynamic properties considered. The effects of the EECs on the static energy are similar in diamond and fcc Al, the larger the more the predicted room conditions volume (and bulk modulus) deviate from the experimental result.

In addition, APBAF and BPSCAL, even though the former uses one adjustable parameter and the latter uses two, almost match for PBE, so it is to be expected that they yield similar results. This is indeed the case for MgO, while for Al and diamond, the divergence is slightly more pronounced. The APBAF correction is therefore a good alternative if the experimental bulk modulus is not available. The good results of this one-parameter correction support the conclusions in Ref. 28.

It is interesting to consider how the correction modifies the infinite pressure ($V \to 0$) and infinite volume limits of the crystal. The contribution of the energy correction vanishes for PSHIFT and APBAF on infinite compression and expansion, respectively. Conversely, the energy contribution diverges unphysically on expansion for the PSHIFT and on compression for the APBAF corrected energies, although in the latter the divergence on compression is slower than that of the raw static energy. Therefore, the correction effects of APBAF essentially vanish in both compression and expansion limits. In the case of BPSCAL, the behavior of the energy and the pressure is that of a scaling on both compression and expansion:

$$\tilde{p}_{\text{sta}}(V) = \frac{B_{\text{expt}}}{B_0} p_{\text{sta}}\left(V \frac{V_0}{V_{\text{expt}}}\right) \tag{21}$$

and the cohesion energy is modified according to Eq. (15).

The energy footing (that is, the energy at the equilibrium volume) of the corrected energies is made to be the same as in the original $E(V)$ curve by adding a constant energy term when necessary. This precaution is important if the EECs are used in the context of comparing energies of different phases

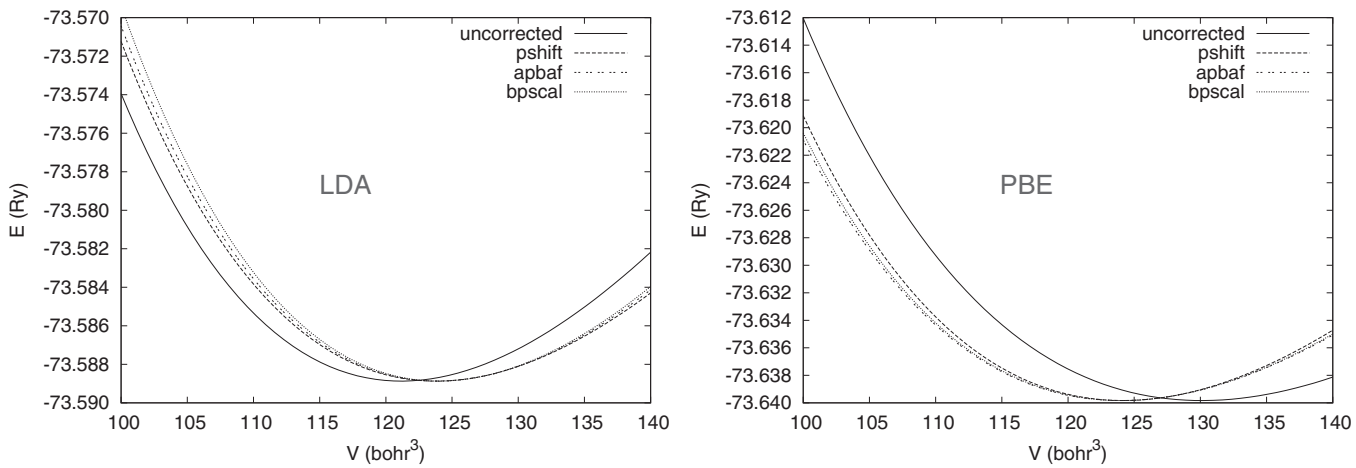

FIG. 1. Uncorrected and corrected static energy curves of magnesium oxide for the LDA (left) and PBE (right) exchange-correlation functionals.

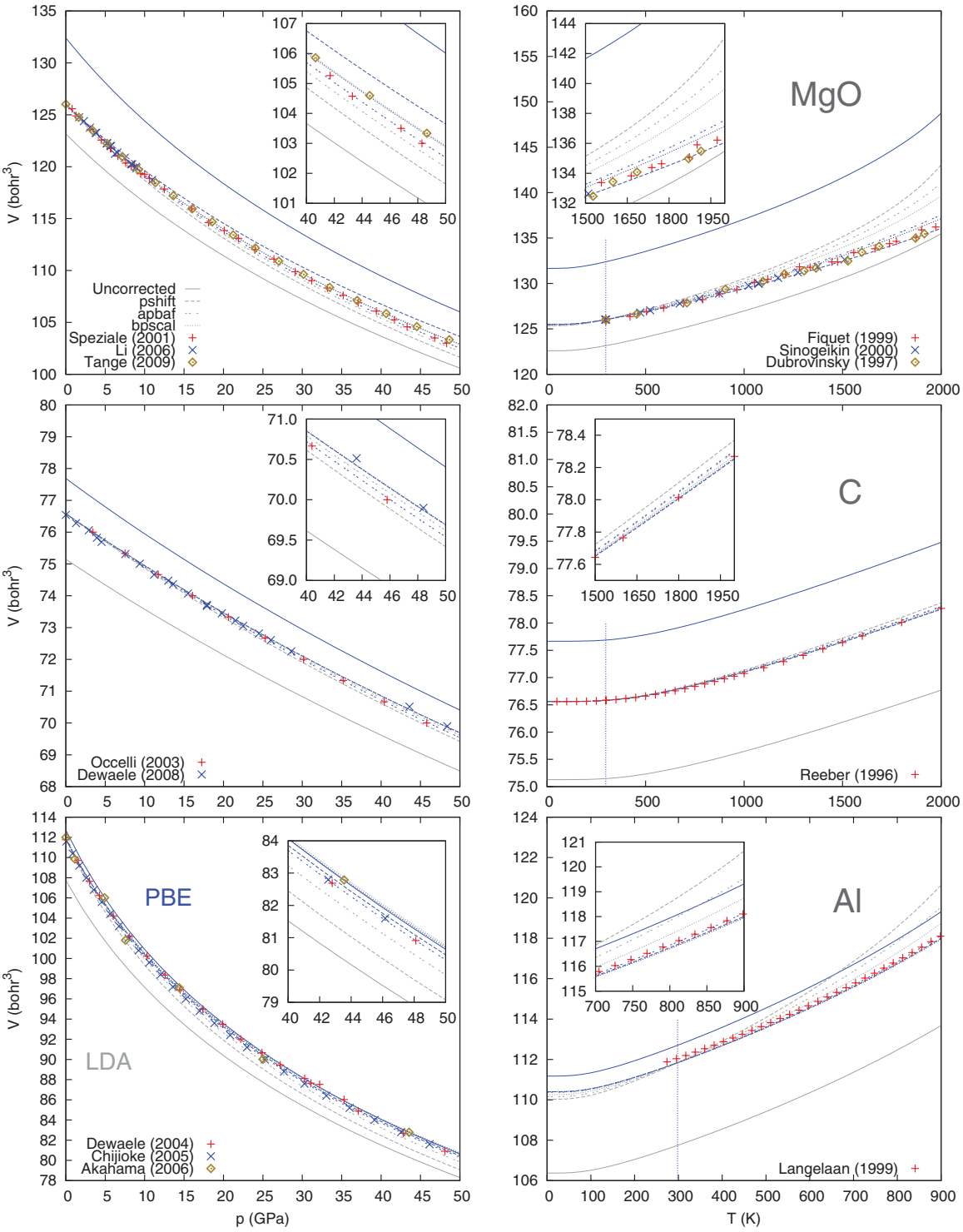

FIG. 2. (Color online) The pressure dependence of equilibrium volume at $T^0 = 298.15$ K (left) and the thermal expansion curve at zero pressure (right) are shown for the three systems under study. Relevant experimental data (or fits to experimental data) are included. The labels correspond to the first author and year of publication of Refs. 37,38,40,43–52. The insets show a zoom on the high-temperature and high-pressure regions of the graph. The room temperature is marked by a vertical line in the right pane plots.

of the same solid, as is the case in the computation of phase diagrams.

Figure 2 shows the performance of the EECs in the calculation of the equation of state of the examined solids. As a reference, we use some of the latest experimental results. The uncorrected LDA and PBE curves bracket the experimental $V(p)$ and $V(T)$ with the typical overbinding and underbinding behaviors. A direct conclusion of these results is that, because of the systematic errors caused by the choice of the exchange-correlation functional and the lack of a systematic way of

improving the results, *it is not possible to blindly predict the equation of state of a simple solid using the uncorrected data alone*. This observation extends to other thermodynamic properties, as shown below and in the literature.[6]

Regarding the corrected EOS, all the EECs yield approximately the same result in the low-temperature–low-pressure regions, and deviate for more extreme conditions. This observation is easily explained: all EECs correct the $V(p=0,T^0)$ datum to V^0_{expt}, which corresponds to the leftmost point of the $V(p)$ graph, and to the point represented by a vertical dotted line in the $V(T)$ graph. In the case of the BPSCAL correction, the slope of $V(p)$ at the same point is also fixed by the experimental bulk modulus.

The $V(p)$ plots show that the transferability of p/B_0 versus V/V_0 among LDA and PBE functionals is preserved when zero-point and thermal effects up to 298.15 K are included. The BPSCAL corrected isotherms for both functionals agree to less than 0.09 bohr^3 in a range that extends up to 250 GPa. This coincidence worsens on increasing the temperature due to anharmonic effects. The PSHIFT correction is, in general, the EEC whose agreement with experimental results is worse. The PSHIFT corrected volumes show the same tendency to systematic overbinding and underbinding errors than the source LDA and PBE functionals, respectively, although on a much smaller scale. The APBAF LDA result is slightly overbinding. Also, it is not possible to choose from APBAF PBE and both BPSCAL results on grounds of a comparison to experimental data alone in these solids. The volumes predicted by APBAF PBE are systematically (although only slightly) smaller than both BPSCAL results.

The zero-pressure thermal expansion curves $V(T)$ provide a more critical test for the EECs, not only because the volume range spanned is smaller, but also because of the inevitable breakdown of the quasiharmonic approximation at high temperatures.[53] In this sense, the volume expansion curves shown in Fig. 2 are the worst-case scenario[26] because the relevance of anharmonic effects decreases on increasing the external pressure. This observation is important in the context of generating reliable results for geophysical applications where, because of the extreme pressure and temperature conditions, no direct experimental confirmation is possible. The corrected $V(T)$ results are coincident to experimental accuracy at low temperatures, with the PSHIFT correction roughly bracketing the other curves.

In the high-temperature region, the calculated EOS, with independence of the correction, show a marked deviation from the experimental result at a given temperature, readily explained by the lack of intrinsic anharmonic contributions. The temperature at which this effect starts to become important, however, depends slightly on the EEC and heavily on the functional and the solid. For the systems studied, MgO ($T^0_m = 3125$ K) shows the anharmonic effect at the lowest temperature.[53] In the case of diamond ($T^0_m = 3820$ K), these contributions are relatively unimportant up to 2000 K. The case of aluminum is particularly surprising because of the agreement with experimental $V(T)$ up to temperatures very close to the melting point $T^0_m = 933.47$ K. The temperature for the onset of intrinsic anharmonic effects seems to be higher for the PBE functional than for LDA, an effect that is observed for other thermodynamic properties as well (Sec. V). The APBAF EEC shows the deviation effect slightly sooner than BPSCAL. The PSHIFT PBE curve has the wider temperature range of agreement with experiment thanks to error cancellation.

Summarizing, the results of Fig. 2 show that, at least for the studied systems, *it is possible to generate reliable equations of state that rival in accuracy with experimental results using first-principles calculations corrected with one or two easily accessible experimental data*. Of course, the calculated EOS are valid as long as the prediction is not extended beyond the limit of validity of the quasiharmonic approximation. In our opinion, this is an important result because it makes it possible to generate reliable $V(p,T)$ data for pressures and temperatures that can not be accessed experimentally, and not merely a bracket of the correct result. The unsolved problem of selecting or designing an accurate exchange-correlation functional is avoided in practice by a simple and feasible scaling. Furthermore, the correction schemes are applicable to any regular solid and to any functional.

We can extract some insights about the suitability of functionals in the calculation of equations of state. The results of Fig. 2 show that LDA meets the limit of validity of QHA sooner than PBE. This conclusion and the fact that, according to Fig. 1, corrections to the exchange-correlation functionals present systematic trends, suggest that there is an underlying physical explanation at DFT level, and that the static energy corrections presented here can be reformulated as an additional term of the DFT Hamiltonian.[13] We will not delve further into theoretical considerations in this paper, but a more detailed study examining the variation of the correction parameters with chemical environment in crystals is, in our opinion, definitely worthwhile.

B. Pressure-volume-temperature equations of state

Given the excellent agreement with experimental $V(p)$ and $V(T)$ data, we can now propose p-V-T equations of state based on our theoretical predictions for MgO, diamond, and Al using the PBE results corrected with the BPSCAL EEC, the best scheme according to Fig. 2. The analytic formulation of the $p(V,T)$ we use is one of the Mie-Grüneisen-Debye expressions proposed in the work by Tange *et al.*[44]:

$$p(V,T) = p_{T_0}(V) + \Delta p_{\text{th}}(V,T), \tag{22}$$

with $p_{T_0}(V)$ the reference isotherm at temperature T_0 and Δp_{th} the thermal pressure. The former can be chosen as one of the usual low-order EOS popular in the literature. The latter is defined as

$$\Delta p_{\text{th}}(V,T) = \frac{3nR\gamma}{V}\left[D_3(\theta_D/T) - D_3(\theta_D/T_0)\right], \tag{23}$$

where n is the number of atoms per cell, $D_n(x)$ is a Debye integral

$$D_n(x) = \frac{n}{x^n}\int_0^x \frac{t^n}{e^t - 1}dt, \tag{24}$$

and the Debye temperature and Grüneisen parameter depend on volume according to

$$\gamma(V) = \gamma_0\{1 + a[(V/V_0)^b - 1]\}, \tag{25}$$

$$\theta_D(V) = \theta_0 \left(\frac{V}{V_0}\right)^{\gamma_0(a-1)} \exp\left[\frac{\gamma_0 - \gamma(V)}{b}\right]. \quad (26)$$

The adjustable parameters in the equations above are those of the reference isotherms θ_0, γ_0, a, and b.

Although the functional form of this $p(V,T)$ equation is equivalent to that of Tange *et al.*, the intent is different. In their work, the parameters were obtained by a careful fitting to the available $V(p)$, $V(T)$, $B_S(p)$, and $B_S(T)$ experimental data, with the purpose of extrapolating the behavior of the crystal to any pressure and temperature. In this work, we generate a $V(p,T)$ grid for the fitting procedure using the PBE results and the BPSCAL energy correction for a wide range of pressures (0 to 500 GPa) and temperatures (0 to 3000 K, except for Al, where the upper limit is 800 K). Given an arbitrary volume and temperature within the explored range, our expression interpolates the pressure using the actual calculated values.

Regarding the technical details of the fit, we find that the EOS described by Eqs. (22)–(26) is the p-V-T equation, which best represents our results of the three options proposed in Ref. 44. Our numerical tests indicate that the reference isotherm $p_{T_0}(V)$ is better represented using a third-degree polynomial in the Eulerian strain (f):

$$p(f) = \sum_{k=0}^{3} c_k f^k, \quad (27)$$

where f is defined as

$$f = \frac{1}{2}\left[\left(\frac{V_{\text{ref}}}{V}\right)^{\frac{2}{3}} - 1\right], \quad (28)$$

and V_{ref} is a reference volume, possibly but not necessarily the static equilibrium volume. The fitting of the p-V-T equation of state is much improved by using the coldest isotherm available ($T_0 = 0.0001$ K) rather than the room-temperature isotherm, the sensible choice for an experimental study. The quality of the fit is insensitive, up to physical precision, to the fineness and shape of the grid.

As expected from the previous analysis, we find that it is necessary to exclude the regions where anharmonic effects are important. To this end, we use an exclusion criterion based on the approximate Debye temperature of a crystal, calculated as in Refs. 31 and 29:

$$\Theta_D(V) = \frac{1}{k_B}(6\pi^2 V^{1/2} n)^{1/3} f(\sigma) \sqrt{\frac{B_{sta}}{M}}, \quad (29)$$

where M is the cell molecular mass and σ is the Poisson ratio, which, for simplicity, we assume to be 0.25, the value of a Cauchy solid. For a given pressure p and temperature T, a point of the fitting grid is excluded if 1.5 times the Debye temperature at the volume associated to p via the cold isotherm $[V(p,T_0)]$ is smaller than T. The ablated regions are represented in Fig. 3. Because of its sound physical foundation, we expect the p-V-T equation to correctly extrapolate to the high-temperature regions.

The fitted p-V-T EOS parameters are presented in Table III. The mean error and the maximum deviation in the predicted pressure are always smaller than 0.1 and 0.5 GPa, respectively. The fitted $p(V,T)$ expression is a faithful representation of the original first-principles data in the fitted region, and the interpolation error is expected to be of the order of, and approximately bound by, these values.

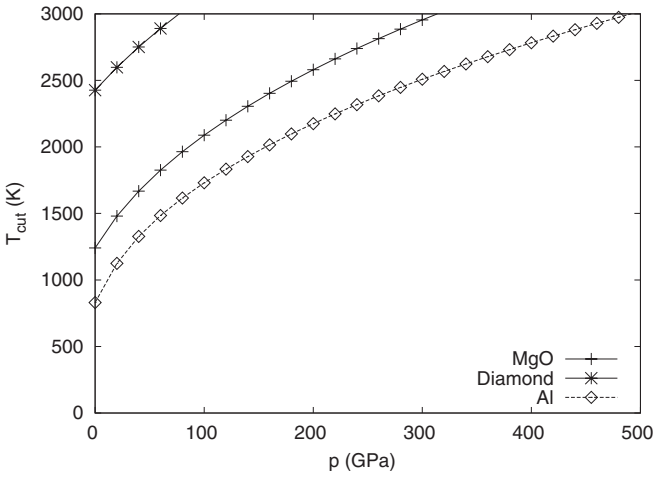

FIG. 3. Pressure-dependent temperature limit where the fitting grid for the p-V-T equation of state is sectioned. The region above the curves is not fitted for the corresponding system.

In the particular case of the equation of state of MgO (Ref. 21 and references therein), relevant because of its use as pressure calibrant, Tange *et al.*[44] use as an additional criterion a comparison of the predicted adiabatic bulk moduli $B_S(p,T = T^0)$ and $B_S(p = 0,T)$ from previous experimental studies on MgO. For the sake of comparison, Fig. 4 presents the calculated and experimental $B_S(p)$ and $B_S(T)$ curves for magnesium oxide. Again, the coincidence with the experimental results is very good, considering that only two experimental data are used for the empirical correction. We must note that, from the technical point of view, B_S is a quantity considerably more difficult to access than the isothermal bulk modulus B_T:

$$B_S = B_T + \frac{C_v \gamma^2 T}{V}, \quad (30)$$

with C_v the constant volume heat capacity. The reason is that it involves the Grüneisen parameter, which is calculated as a volume derivative of the entropy

$$\gamma = \frac{V}{C_v}\left(\frac{\partial S}{\partial V}\right)_T. \quad (31)$$

V. CORRECTED THERMODYNAMIC PROPERTIES

A. Calculated properties at ambient conditions

We now turn to the analysis of the effect that the empirical corrections have on the calculated thermodynamic properties. Table IV presents the properties obtained at ambient conditions from the raw and corrected QHA data. Given the abundance of experimental data, we extend the comparison to 0 GPa and 1000 K conditions for MgO. The error bars calculated by using strain polynomial statistics[24,25] are included in the comparison. We must note, however, that these error bars measure only the precision of the predicted values regarding the fit, not the underlying DFT calculation itself.

TABLE III. Fitting parameters of the p-V-T equation of state expression given by Tange *et al.* (Ref. 44) [Eqs. (22)–(26)]. Because of the strong correlation between the thermal pressure coefficients (θ_0, a, b, γ_0), it was not possible to fit the complete expression to the diamond EOS, so we chose to fix $a = 1$. The maximum and average absolute deviations in the predicted pressure are shown in the last two entries. The reference temperature is $T_0 = 0.0001$ K for the three systems.

	MgO	Aluminum	Diamond
V_{ref} (bohr^3)	125.4823	110.5957	76.5627
c_0 (GPa)	2.9756546×10^{-2}	$-6.1364390 \times 10^{-2}$	1.6119952×10^{-3}
c_1 (GPa)	$4.9563449 \times 10^{+2}$	$2.3967089 \times 10^{+2}$	$1.3369808 \times 10^{+3}$
c_2 (GPa)	$2.5844813 \times 10^{+3}$	$1.4144945 \times 10^{+3}$	$6.2102976 \times 10^{+3}$
c_3 (GPa)	$4.1650008 \times 10^{+3}$	$1.6937468 \times 10^{+3}$	$5.8403959 \times 10^{+3}$
θ_0 (K)	857.8250	410.7608	2241.0368
γ_0	1.5302605	2.1956944	1.0141375
a	0.48012896	0.69482331	1 (fixed)
b	2.2555157	1.9957874	0.92715790
$\lvert\Delta p\rvert_{\text{max}}$ (GPa)	0.292	0.275	0.437
$\lvert\Delta p\rvert_{\text{avg}}$ (GPa)	0.0754	0.0487	0.0923

As in the case of the equation of state, the BPSCAL correction to PBE obtains an excellent agreement with the experimental properties of the three systems under consideration, shifting the calculated properties in the direction of the experimental results and eliminating the systematic trend in the uncorrected PBE. We show later that this agreement extends to wider regions of pressure and temperature. Let us examine the various properties presented in the table.

Regarding the calculated equilibrium volume and bulk modulus, the uncorrected results show the typical overbinding and underbinding behaviors of LDA and PBE, respectively. In the corrected results, the parameters are chosen so that the room-temperature volume is reproduced. The match is not exact because of numerical errors caused by the fitting procedure, but the room-temperature volumes agree with experiment within the range of physical significance. In the case of MgO at 1000 K, the corrected LDA and PBE results diverge, although the gap between both figures is smaller if a correction is applied.

An important observation is that, when the volume is corrected, LDA tends to overestimate the volume of MgO at 1000 K while PBE underestimates it, the exact opposite of the uncorrected tendency. The table shows that this inversion of the relative behavior of LDA and PBE and the reduction of the gap between them is a general feature of the corrected results and extends to higher temperatures at zero pressures, according to the figures in the next section. The corrected PBE results tend to be closer to experiment than LDA, which, depending on the property, slightly overestimates (volume) or underestimates (bulk modulus) the correct result. These observations agree with previous results on the pressure shift correction, where the LDA and PBE inversion were observed.[12]

For the isothermal bulk modulus, only the BPSCAL corrected values are forced to agree with the experimental datum. The inversion of the LDA and PBE bulk moduli on the correction described above is observed again: LDA predicts smaller B_T than PBE, the latter being, in general, in closer agreement with experiment.

It is interesting to note that when the PSHIFT EEC is considered, the corrected PBE results offer a much better prediction of the B_T of the three systems than the LDA result. This is in sharp contrast to van de Walle and Ceder arguments in favor of the corrected LDA.[13] The discrepancy may tentatively be ascribed to the lack of zero-point and thermal effects in their work, which cause a non-negligible softening of the isothermal bulk modulus, and are therefore essential to compare with experimental data. The APBAF correction tends to predict an isothermal bulk modulus smaller than the experimental result, slightly higher and in better accordance to the latter in the case of PBE, except in diamond.

Similar considerations apply to the adiabatic bulk modulus, closely related to B_T, and to the pressure derivatives B_T' and B_T''. The inversion of the LDA and PBE results is still observed, and the BPSCAL result is closer to the experimental result as a consequence of having fixed the B_T, except in diamond, where due to the extremely high bulk modulus, errors in the experimental data cause it to be inconsistent. Indeed, according to Eq. (30), it must hold that $B_S > B_T$ and, similarly, $C_p > C_v$, but experimental errors in different experimental sources make the data of diamond in Table IV violate these inequalities. On the other hand, B_T' and B_T'' quantities can be calculated robustly thanks to our fitting technique.[24,25] The calculated error bars allow us to conclude that B_T' and B_T'' can be reliably predicted, but that successive pressure derivatives of the bulk modulus are not available using the raw static volume grid.[28] We observe in the table that the general tendency for all the properties is that PBE error bars are slightly smaller than LDA ones. In the case of MgO, increasing the temperature enlarges the error bars of all calculated properties.

The volumetric thermal expansivity is mainly dependent on the product of volume and isothermal bulk modulus (its *physical hardness*, see Ref. 28 and references therein):

$$\alpha = \frac{C_v \gamma}{V B_T}. \tag{32}$$

The raw LDA results closely agree to the experimental α values, and all the corrections go in the wrong direction causing a significant overestimation. This is different from the PBE behavior, where all the corrections and, in particular, BPSCAL, effectively correct the error in the raw values, resulting in a good agreement with the measurements.

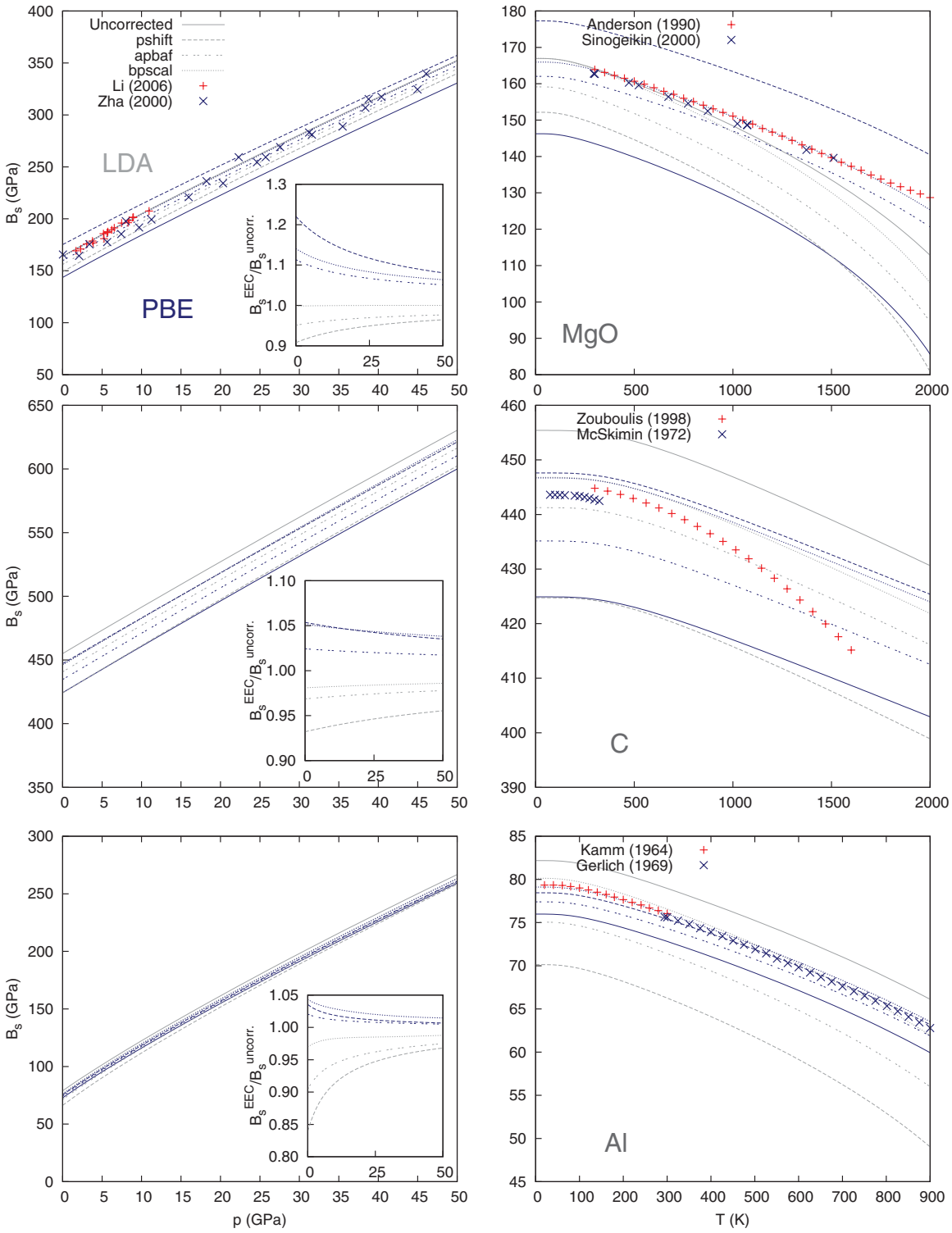

FIG. 4. (Color online) The dependence of the adiabatic bulk modulus (B_S) with pressure at room temperature (left) and with temperature at zero pressure (right) for MgO, diamond, and Al, calculated using different functionals and empirical energy corrections. Experimental results, when available, are included and labeled using the first author and year (Refs. 37,46,54,58–62).

Uncorrected LDA and corrected PBE predict that values of α are close to the experimental result, while LDA results corrected to the experimental volume overestimate the quantity.

In contrast to volume and elastic properties, the effects of the empirical corrections on the thermodynamic quantities that do not depend directly on the static energy are more subtle, namely, F_{vib} and S, their volume derivatives p_{th} and γ, and the heat capacities C_v and C_p. For these quantities, thermal effects at 300 K are small enough to give a good agreement with experiment, irrespective of functional and correction.

TABLE IV. Thermodynamic properties of MgO, diamond, and fcc Al at ambient conditions. In the case of MgO, also $p = 0$ GPa and $T = 1000$ K conditions are considered. Except where noted, the sources of experimental data are Anderson and Zou (Ref. 54) for MgO and the fit to experimental data by Jacobs *et al.* (Ref. 55) for Al. The empirical data used for the corrections are emphasized in boldface. The values for the thermal pressure in italics have been calculated indirectly (Ref. 54).

	Uncorrected		PSHIFT		APBAF		BPSCAL		Expt.	Ref.
	LDA	PBE	LDA	PBE	LDA	PBE	LDA	PBE		
					MgO, 298.15 K, 0 GPa					
V (bohr^3)	123.156(50)	132.389(34)	126.027(63)	126.022(11)	126.025(55)	126.025(21)	126.024(54)	126.024(18)	**126.025**	37
$F_{\rm vib}$ (kJ/mol)	11.2266(122)	9.9572(71)	10.5571(143)	11.4267(29)	10.5575(125)	11.4259(53)	10.5578(122)	11.4263(46)		
S (J/mol K)	27.345(23)	29.920(16)	28.680(31)	27.008(6)	28.679(27)	27.010(10)	28.679(27)	27.009(9)	27.18	
$p_{\rm th}$ (GPa)	2.725(69)	2.554(44)	2.706(77)	2.631(14)	2.706(68)	2.627(27)	2.704(67)	2.626(23)	*0.717*	
B_T (GPa)	161.77(67)	140.99(59)	146.44(69)	172.92(51)	153.52(66)	157.54(54)	161.33(68)	161.47(57)	**161.3**	37
B_S (GPa)	164.18(67)	143.56(59)	149.04(69)	175.20(51)	156.12(66)	159.81(54)	163.93(68)	163.75(57)	163.9	
α (1×10^{-5} K)	3.226(14)	3.744(17)	3.689(19)	2.886(9)	3.519(16)	3.168(11)	3.348(15)	3.091(11)	3.12	
C_v (J/mol K)	36.9192(121)	38.1831(80)	37.6329(169)	36.6902(34)	37.6325(150)	36.6912(62)	37.6321(147)	36.6908(54)	36.9	
C_p (J/mol K)	37.4708(143)	38.8793(108)	38.3011(197)	37.1732(43)	38.2698(176)	37.2213(74)	38.2385(171)	37.2080(62)	37.409	
B'_T	4.255(45)	4.296(49)	4.401(67)	4.026(27)	4.292(57)	4.218(34)	4.285(56)	4.202(38)		
B''_T (GPa^{-1})	−0.0369(51)	−0.0474(108)	−0.0474(86)	−0.0272(28)	−0.0416(74)	−0.0355(38)	−0.0393(69)	−0.0336(36)		
γ	1.5534(10)	1.6332(6)	1.6144(14)	1.5297(1)	1.6143(12)	1.5298(3)	1.6143(11)	1.5298(2)	1.54	
					MgO, 1000 K, 0 GPa					
V (bohr^3)	126.972(177)	137.076(172)	130.538(219)	129.444(84)	130.291(205)	129.819(100)	130.053(193)	129.719(95)	129.6	
$F_{\rm vib}$ (kJ/mol)	−32.269(113)	−36.154(106)	−34.707(149)	−31.460(49)	−34.539(141)	−31.701(67)	−34.370(135)	−31.633(64)		
S (J/mol K)	83.471(104)	87.191(101)	85.791(147)	82.730(50)	85.625(138)	82.953(59)	85.464(130)	82.894(56)	82.24	
$p_{\rm th}$ (GPa)	7.327(201)	7.078(163)	7.462(213)	6.976(104)	7.456(203)	6.968(121)	7.441(192)	6.965(116)	*4.96*	
B_T (GPa)	137.17(226)	116.79(170)	118.89(217)	152.94(202)	126.76(215)	136.52(209)	134.79(217)	140.53(215)	141	
B_S (GPa)	148.40(223)	128.36(168)	130.99(214)	163.37(202)	138.79(212)	146.99(201)	146.75(214)	150.99(215)	151.1	
α (1×10^{-5} K)	5.058(87)	5.816(87)	5.980(116)	4.329(58)	5.598(100)	4.853(75)	5.255(89)	4.714(73)	4.47	
C_v (J/mol K)	48.5866(20)	48.7516(36)	48.6831(101)	48.5653(54)	48.6713(87)	48.5718(13)	48.6649(62)	48.5731(12)	47.61	
C_p (J/mol K)	52.563(77)	53.584(82)	53.637(115)	51.876(50)	53.291(98)	52.297(59)	52.985(86)	52.188(58)	50.87	
B'_T	4.935(184)	5.168(378)	5.413(291)	4.348(104)	5.194(269)	4.633(122)	5.122(247)	4.594(120)		
B''_T (GPa^{-1})	−0.106(30)	−0.170(88)	−0.168(55)	−0.064(22)	−0.141(48)	−0.088(28)	−0.126(41)	−0.082(27)		
γ	1.6181(39)	1.7044(35)	1.7013(55)	1.5747(14)	1.6953(12)	1.5803(16)	1.6893(48)	1.5787(15)	1.54	
					Al fcc, 300 K, 0 GPa					
V (bohr^3)	107.744(59)	112.701(49)	111.840(77)	111.840(47)	111.840(69)	111.840(48)	111.836(69)	111.834(46)	**111.840**	40
$F_{\rm vib} + F_{\rm el}$(kJ/mol)	−0.2069(99)	−0.5159(77)	−0.8890(136)	−0.3814(74)	−0.8890(123)	−0.3814(76)	−0.8882(123)	−0.3805(71)		
S (J/mol K)	27.914(28)	28.807(23)	29.865(40)	28.409(22)	29.865(36)	28.409(22)	29.862(36)	28.406(21)	28.234	
$p_{\rm th}$ (GPa)	1.862(23)	1.782(12)	1.890(22)	1.779(16)	1.890(18)	1.779(16)	1.887(20)	1.775(12)		
B_T (GPa)	75.50(62)	69.44(78)	62.41(79)	72.10(73)	67.55(78)	71.01(73)	72.72(69)	72.69(66)	**72.7**	51
B_S (GPa)	79.00(62)	72.84(78)	66.31(79)	75.43(73)	71.45(78)	74.34(73)	76.62(69)	76.02(66)		
α (1×10^{-5} K)	7.042(58)	7.404(83)	8.883(116)	7.077(71)	8.207(97)	7.185(74)	7.624(76)	7.019(65)	6.986	
C_v (J/mol K)	23.1549(46)	23.3024(38)	23.4466(50)	23.2357(37)	23.4466(45)	23.2357(38)	23.4463(45)	23.2352(35)	23.288	
C_p (J/mol K)	24.2282(119)	24.4440(147)	24.9121(237)	24.3102(122)	24.8006(200)	24.3266(126)	24.7039(170)	24.3009(121)	24.285	
B'_T	4.874(126)	4.936(104)	5.354(101)	4.847(117)	5.099	4.890(91)	5.005(73)	4.920(86)		
B''_T (GPa^{-1})	−0.143(18)	−0.174(36)	−0.244(50)	−0.157(29)	−0.197(43)	−0.163(30)	−0.172(31)	−0.158(24)		
γ	2.2078(20)	2.2191(16)	2.3600(30)	2.1917(15)	2.3600(27)	2.1917(15)	2.3598(27)	2.1915(14)	2.14	
					Diamond, 300 K, 0 GPa					
V (bohr^3)	75.1502(32)	77.6898(52)	76.5804(31)	76.5805(55)	76.5809(33)	76.5809(58)	76.5807(28)	76.5826(61)	**76.581**	38
$F_{\rm vib}$ (kJ/mol)	34.7745(15)	33.8764(23)	34.0881(15)	34.3763(27)	34.0879(16)	34.3761(29)	34.0880(13)	34.3753(30)		
S (J/mol K)	4.7361(4)	4.9954(7)	4.9224(4)	4.8501(7)	4.9225(4)	4.8502(8)	4.9225(4)	4.8504(8)	4.7240	56
$p_{\rm th}$ (GPa)	5.344(7)	5.116(42)	5.194(5)	5.232(48)	5.197(6)	5.235(46)	5.196(8)	5.244(49)		
B_T (GPa)	454.64(20)	424.11(53)	423.89(27)	446.84(32)	440.43(24)	434.37(29)	445.98(25)	445.92(42)	**446**	38
B_S (GPa)	454.97(20)	424.48(53)	424.25(27)	447.18(32)	440.79(24)	434.72(29)	446.34(25)	446.27(42)	444.8	57
α (1×10^{-5} K)	0.3135(2)	0.3567(4)	0.3534(2)	0.3268(2)	0.3402(2)	0.3362(2)	0.3359(2)	0.3275(3)	0.3051	49
C_v (J/mol K)	12.2959(10)	12.8737(15)	12.7224(9)	12.5459(17)	12.7225(10)	12.5460(18)	12.7225(8)	12.5465(18)	12.321	49
C_p (J/mol K)	12.3049(10)	12.8849(15)	12.7332(9)	12.5556(17)	12.7329(10)	12.5560(18)	12.7327(8)	12.5563(19)	12.218	56
B'_T	3.676(14)	3.668(63)	3.759(14)	3.618(57)	3.691(13)	3.662(57)	3.677(11)	3.674(57)		
B''_T (GPa^{-1})	−0.0090(5)	−0.0094(18)	−0.0108(11)	−0.0075(20)	−0.0097(10)	−0.0081(21)	−0.0094(10)	−0.0071(29)		
γ	0.777547(6)	0.81464(9)	0.80475(6)	0.79538(9)	0.80476(6)	0.79539(10)	0.80476(5)	0.79542(10)		

From Table IV, we can therefore conclude that the accuracy in the calculated properties is dominated by volume and static energy effects, either directly (V, B_T, B_S, B'_T, B''_T, α) or indirectly via the correction on the p-V-T equation of state ($F_{\rm vib}$, S, C_v, C_p). When the correct room-temperature volume is enforced by modifying the static energy in any of the EEC schemes, the deviations from the experimental results are smaller and have sign opposite to the uncorrected deviations: if the uncorrected result underestimates a property, then the corrected value overestimates it, and *vice versa*. The corrected PBE results improve, in general, over LDA, and the agreement to experiment using PBE plus BPSCAL is excellent.

B. Pressure and temperature dependence of selected thermodynamic properties

In this section, we examine the effects of the EECs on some important thermodynamic properties by analyzing

their evolution with pressure at room temperature and with temperature at zero pressure. Our objective is inferring the behavior of these properties at arbitrary temperatures and pressures by extrapolation.

Figure 4 shows the pressure and temperature dependence of the calculated adiabatic bulk modulus. The corrected and uncorrected $B_S(p)$ curves are almost parallel to each. They are also nearly linear with pressure, the behavior expected of this quantity. As a consequence, in the case of the calculation of $B_S(p)$, it is essential to fix the correct bulk modulus in the empirical correction, i.e., using BPSCAL, to obtain an accurate result at an arbitrary pressure. If the BPSCAL correction is used, the curves for LDA and PBE match almost exactly.

In magnesium oxide, where the experimental $B_S(p)$ is available, uncorrected LDA and both BPSCAL coincide with the low-pressure data by Li *et al.*[37] and with Zha *et al.*,[58] although the experimental error in the latter is larger and encompasses all the predicted results. No experimental data were found for the pressure dependence of the B_S in aluminum and diamond, but consistence is maintained: in all three systems, the BPSCAL correction brings LDA and PBE to coincidence.

The inset of Fig. 4 shows the pressure evolution of the quotient between the corrected B_S and the one obtained with the uncorrected data. The correction on B_S is maximum at zero pressure and decays slowly on compression for all the EECs considered. The correction works systematically yielding smaller bulk moduli in LDA and larger B_S in PBE, hence, correcting their systematic trends. The corrections imposed by the EECs that do not explicitly fix the isothermal bulk modulus (PSHIFT and APBAF) are in the same direction as BPSCAL, although their predicted values are slightly different.

The $B_S(T)$ curves corresponding to different EECs are widely different, but again the two BPSCAL corrected curves are very close to each other, diverging only at high temperatures. The most striking feature of the $B_S(T)$ plots is the spectacular agreement between the BPSCAL plus PBE results and the experimental predictions. Again, in the case of diamond, no reliable experimental sources for the comparison exist given the difficulty involved in obtaining accurate bulk moduli for a system of such hardness. Indeed, the low-temperature $B_S(T)$ data by McSkimin *et al.*[60] could be reproduced by using a different B_T as a parameter for the BPSCAL EEC, although we have chosen to maintain the parameter in Table II for consistency. The high-temperature $B_S(T)$ by Zouboulis *et al.*[59] is calculated by combining the $c_{ij}^S(T)$ obtained using a Brillouin scattering technique, the results showing strong experimental noise. Indeed, the fitting coefficient for the T^2 term of $B_S(T)$ cited by the authors contains less than two significant digits. Given the excellent agreement in the prediction of the other thermodynamic properties, we can conclude that the cited data are suspicious, and more accurate experiments to determine the high-temperature adiabatic bulk modulus of diamond are required in order to perform a sensible comparison.

Regarding the rest of the EECs, the empirical corrections push the curves in opposite directions: they make the crystal softer for LDA and stiffer for PBE, the same as observed for $B_S(p)$. However, only when BPSCAL is used, the experimental $B_S(T)$ curve is predicted accurately, thanks to the additional correction parameter.

A further feature, especially visible in the case of MgO, is the unphysical softening of $B_S(T)$ at high temperatures. This deviation from the expected physical behavior is caused by the lack of intrinsic anharmonic effects, and can be observed as well in $C_p(T)$ and $\alpha(T)$ (Fig. 5) and in the deviations of the experimental $C_v(T)$ data from the classical Dulong-Petit limit predicted by the quasiharmonic theory (Fig. 6). The temperature at which the lack of anharmonic effects is apparent is lower for LDA than for PBE and depends on a smaller scale of the EEC used, effectively extending the range of applicability of PBE to higher temperatures than LDA. This effect is also observed for the thermal expansion (Fig. 2), although on a smaller scale.

Figure 5 represents the calculated and experimental constant pressure heat capacity and thermal expansivity. It is clear from these plots that the application of EECs affects the temperature region where the quasiharmonic approximation can be applied. A temperature limit of this range has been proposed by Wentzcovitch *et al.*[74] as the temperature at which the thermal expansivity acquires superlinear (that is, unphysical) behavior, and the curvature $d^2\alpha/dT^2$ changes from negative (low T) to positive (high T). In our test systems, this effect is observed clearly in MgO and Al, although in the latter, only at temperatures close to the melting point. We should note, however, that the temperature range where the calculated volumes are accurate is larger than for α, which, being related to the temperature derivative of the volume, is more sensitive to anharmonic effects on the thermal expansion of the crystal. The quality of the predicted $C_p(T)$ and $\alpha(T)$ is excellent, rivaling with the experimental accuracy within the validity range of QHA. We note, again, that this range is larger for the PBE than for the LDA functional and that the effect of the EECs is opposite on both. In the PBE results, EECs flatten the $\alpha(T)$ and $C_p(T)$ curves at higher temperatures, in the order APBAF< BPSCAL < PSHIFT, while the behavior for LDA is exactly the opposite: the corrected LDA results deviate sooner from the correct behavior than the uncorrected ones, restricting its temperature range of the functional.

An important word of caution is necessary at this point. If uncorrected $B_S(T)$, $C_p(T)$, and $\alpha(T)$ are considered alone,[6,12] the impression one receives is that LDA offers a better prediction of those quantities according to experiment, which perhaps explains the puzzling popularity of LDA in first-principles calculations for geophysics.[53,76] From the figures above, it is clear that this apparent agreement stems from the cancellation of the LDA overbinding with the softening caused by the breakdown of the QHA. When volume corrections are applied, the good performance of LDA vanishes and corrected PBE improves even on the original uncorrected LDA. The EECs we propose avoid relying on dangerous error cancellations, when, as in the case of geophysical applications, the theoretical predictions need to be used in regions of pressure and temperature uncharted by experiments.

When the PBE functional is considered alone, Figs. 2 to 5 show that the APBAF correction performs slightly worse than BPSCAL owing to the reduced number of parameters,

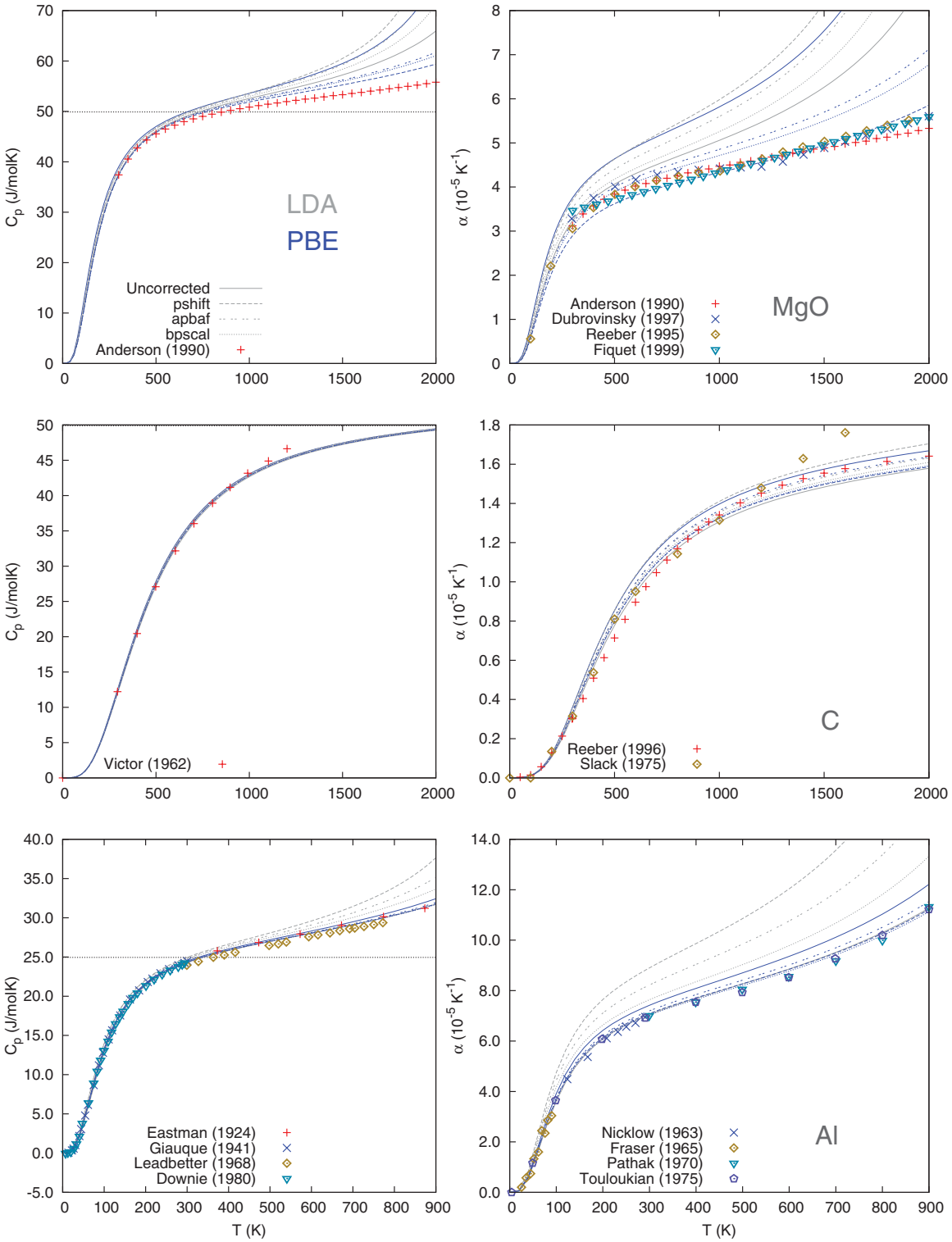

FIG. 5. (Color online) The calculated temperature dependence of the constant pressure heat capacity (C_p, left) and the thermal expansivity (α, right) at zero pressure for the three systems under study. Experimental results correspond to Refs. 45, 47, 54, and 63–73. The Dulong-Petit limit is represented as a dotted horizontal line in the left pane.

but much better than PSHIFT. This is not surprising because the APBAF correction is designed to correct systematic errors in approximate density functionals.[28] The good results obtained confirm the soundness of this correction. In summary, APBAF is a good alternative when only the experimental room-temperature volume, but not the bulk modulus, is known.

Finally, Fig. 6 compares the constant volume heat capacity of the three systems with experimental results. The coincidence at low temperatures is excellent. At higher temperatures, the

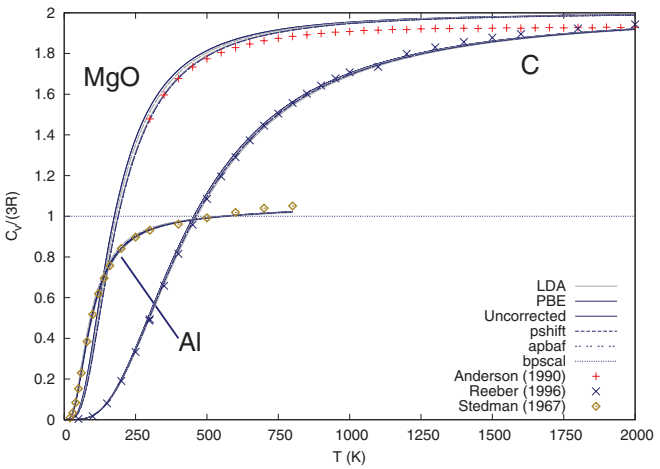

FIG. 6. (Color online) The calculated and experimental constant volume heat capacity (C_v) for MgO, diamond, and Al at zero pressure. Experimental results were obtained from Refs. 49,54,75.

experimental results exceed the Dulong-Petit limit due to intrinsic anharmonicity and, in the case of aluminum, also because of the electronic contribution. Because of the limits imposed by the harmonic approximation on the shape of $C_v(T)$, there is little difference in using different functionals or empirical corrections. The $C_v(T)$ of aluminum contains the electronic contributions that allow it to overstep the classical limit.

C. Impact of the empirical energy corrections on phase stability

An important application of QHA is the calculation of phase diagrams. Phase stability is controlled by the value of the Gibbs free energy G of the different phases of the same solid. The calculation of accurate values of G is therefore an important task in order to obtain reliable phase diagrams, especially considering the minute energy differences often separating the stable geometry from the metastable phases. Typically, there is a relative abundance of data for the stable phase, but metastable phases may or may be not accessible to current experimental techniques. In this situation, it is possible that experimental data to feed the EECs are not available, or available at pressures and temperatures different from ambient conditions. In the second case, we note that the empirical corrections analyzed in this paper can be easily extended to fit experimental data at arbitrary pressure and temperature conditions. On the other hand, if there is absolutely no data from which to draw the correction coefficients, then these coefficients can be transferred from the stable phase. Although a proper validation of this transfer is necessary, van de Walle *et al.*[13] found that the correction pressure in the PSHIFT scheme can be approximated as a weighted average of atomic pressures. We are currently studying the viability of EECs in the determination of transition pressures and phase diagrams. We have shown in a previous paper[21] that the BPSCAL EEC corrects the transition pressures and the phase diagram of MgO, bringing LDA and PBE results to coincidence within 5 to 10 GPa, in contrast with the ≈ 40 GPa uncorrected gap. This result is encouraging, although more adequate systems need to be studied.

A precise value of $G(p,T)$ is essential for a correct ordering of the stability of the different phases entering a phase diagram. Figure 7 shows the corrections to the calculated Gibbs free energy as determined by the three EEC schemes $\Delta G_{\rm EEC}$. This $\Delta G_{\rm EEC}$ is composed of three terms:

$$\Delta G_{\rm EEC}(p,T) = \Delta E_{\rm sta} + p\Delta V + \Delta F_{\rm vib}, \tag{33}$$

where

$$\Delta E_{\rm sta} = E_{\rm sta}[V_{\rm EEC}(p,T)] - E_{\rm sta}[V_{\rm raw}(p,T)], \tag{34}$$

$$\Delta F_{\rm vib} = F^*_{\rm vib}[V_{\rm EEC}(p,T);T] - F^*_{\rm vib}[V_{\rm raw}(p,T);T], \tag{35}$$

$$p\Delta V = p[V_{\rm EEC}(p,T) - V_{\rm raw}(p,T)]. \tag{36}$$

The EEC subscript designates the volume calculated via the corrected static energy, while raw is the uncorrected result. The three contributions to G depend on the volume and, therefore, on the accuracy of the equation of state. In the case of the third term $p\Delta V$, this contribution is directly volume dependent. In the other two cases, the volume correction enters the equation indirectly, via $E_{\rm sta}$ or $F_{\rm vib}$. The three contributions are shown in Fig. 7, together with the total $\Delta G_{\rm EEC}$.

The figure shows that the empirical energy corrections applied to LDA and PBE have opposite signs on all the examined pressure-temperature ranges, which is consistent with the observations for other thermodynamic quantities.

Regarding the $\Delta G_{\rm EEC}(p)$ curve at room temperature, the corrections increase monotonically for LDA and decrease for PBE, crossing zero at the point, around 5 GPa for the three systems, where $p\Delta V$ balances the other two contributing terms. At higher pressures and $T = T^0$, the correction is dominated by the $p\Delta V$ term, is larger in absolute value, and the three EEC schemes diverge. For the systems considered, the ordering of the magnitude of $\Delta G_{\rm EEC}$ is the same: BPSCAL > APBAF > PSHIFT in the case of LDA and APBAF > BPSCAL > PSHIFT for PBE.

The situation with $\Delta G_{\rm EEC}(T)$ at zero pressure is the opposite: $\Delta G_{\rm EEC}$ is positive for PBE and negative for LDA. The correction increases with temperature, with sign opposite to the effect of increasing the pressure, and in this case with a value determined mainly by $\Delta F_{\rm vib}$. The three EECs provide almost the same correction as a result of the cancellation of $\Delta E_{\rm sta}$ with $\Delta F_{\rm vib}$.

Because $\Delta G(p)$ is dominated at low temperatures by the $p\Delta V$ term, it is essential to choose an empirical energy correction that describes adequately the equation of state in order to obtain accurate values of the Gibbs free energy and, as a result, a faithful phase diagram and transition pressures. Note that even the static transition pressures are affected by the static energy corrections, although only through the $\Delta E_{\rm sta}$ and the $p\Delta V$ terms. The thermal $\Delta F_{\rm vib}$ and the static energy contributions are comparatively small, the former being almost independent of pressure. As a consequence of both diagrams, for an arbitrary pressure and temperature, the correction to G is explained by a competition between the pressure ($p\Delta V$) term and the thermal ($F_{\rm vib}$) contribution, with opposite effects.

The relevance of the EECs on static or room-temperature transition pressures is currently under study. From the literature, it is clear that the choice of exchange-correlation

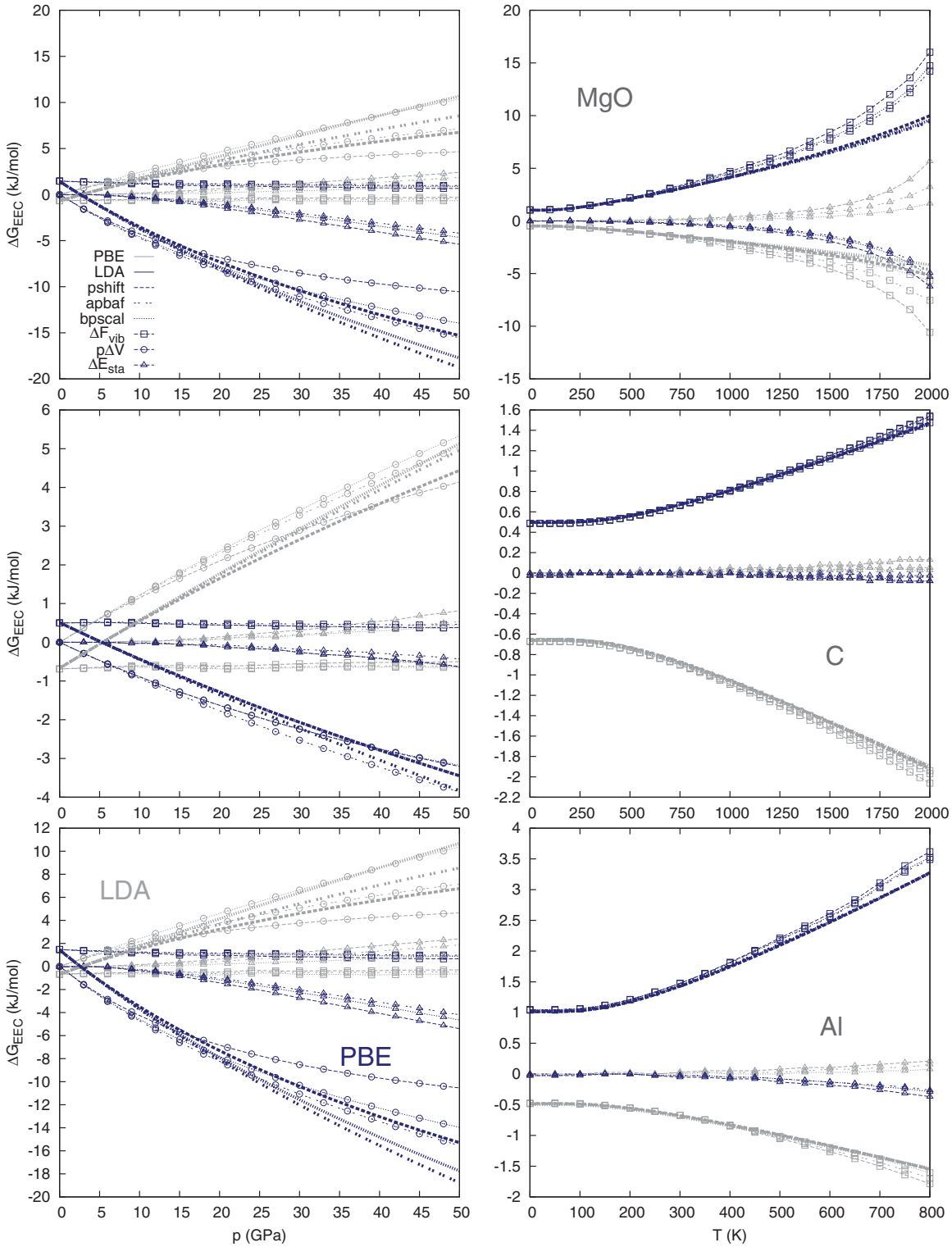

FIG. 7. (Color online) The difference between the corrected Gibbs free energy using the three EEC schemes and the uncorrected G, and the additive terms [Eqs. (34), (35), and (36)] contributing to it are shown. The total ΔG_{EEC} is represented with thick lines, while points have been added to mark each of the curves corresponding to different terms: ΔF_{vib} (squares), $p\Delta V$ (circles), and ΔE_{sta} (triangles). The functionals are represented by line colors: blue for PBE and light gray for LDA. Different line styles correspond to the three empirical corrections used. The left pane contains the pressure evolution of these quantities at room temperature, while the right pane represents their temperature dependence at null pressure. Results are presented for MgO (top), diamond (middle), and aluminum (bottom).

functional affects significantly these quantities,[19,21] and we firmly believe that an appropriate correction to the static energy is in order to improve the agreement with experiment and the predictive power of the DFT quasiharmonic approach.

VI. APPROXIMATE THERMAL MODELS AND COMPLEX SOLIDS

Correcting the static energy using phonon frequencies at each volume can be too onerous in complex solids. In this section, we show how the EECs can be applied with an approximate thermal model to systematically improve the computed EOS, using iron as a test system. In this case, the only piece of information used in the correction will be the static $E(V)$ curve and the experimental parameters, drastically reducing the computational cost of the calculation.

Iron is one of the most studied elements because of its technological and geophysical relevance. Seismological evidence suggests that the Earth's core is composed primarily of iron: liquid in the outer core and solid in the inner core. The actual phase in which iron is present in the inner core is still a subject of debate.[77–80]

Regarding its phase diagram, ferromagnetic body-centered-cubic iron (α-Fe) is stable at room temperature and pressure. At around 15 GPa and with a large hysteresis,[81] the bcc structure transforms into nonmagnetic hexagonal close-packed (hcp) (ε-Fe), which is stable up to the Earth's core pressure. The hcp phase is stable also at high temperatures, but the question of whether it is hcp, double hcp, or a combination of stacking faults that dominates the structure of the inner core still stands.[80] At low pressures and higher temperatures, the γ-Fe phase is found, with face-centered-cubic (fcc) structure.

A challenge in the study of iron is its magnetic structure.[7,82] The bcc phase is stabilized by magnetic interactions,[7,83] which are well reproduced by GGA functionals but not by LDA. Indeed, GGA correctly predicts bcc ferromagnetic to be the stable structure at zero pressure and its transition to nonmagnetic hcp. On the contrary, the energy of the bcc phase in LDA is too high to even compete with closed-packed fcc and hcp structures. The changes in the static energy caused by EECs conserve the energy of the minimum, so the stability order of the magnetic phases is not altered. This is the appropriate behavior because the focus is on correcting volume-related faults of the functional, not errors in the electronic or magnetic treatment of materials.

In the calculations, we use an ultrasoft pseudopotential for Fe with nonlinear core correction and valence configuration $3d^6 4s^2$ with LDA and PBE exchange-correlation functionals. The studied phases are bcc, fcc, and hcp in their ferromagnetic, antiferromagnetic, and nonmagnetic configurations with both functionals, totaling 18 energy-volume curves. The plane-wave energy cutoff was 40 Ry and $\boldsymbol{k}$-point meshes were $20 \times 20 \times 20$ for cubic structures and $14 \times 14 \times 14$ for hcp, ensuring a convergence to the mRy or better in the total energy.

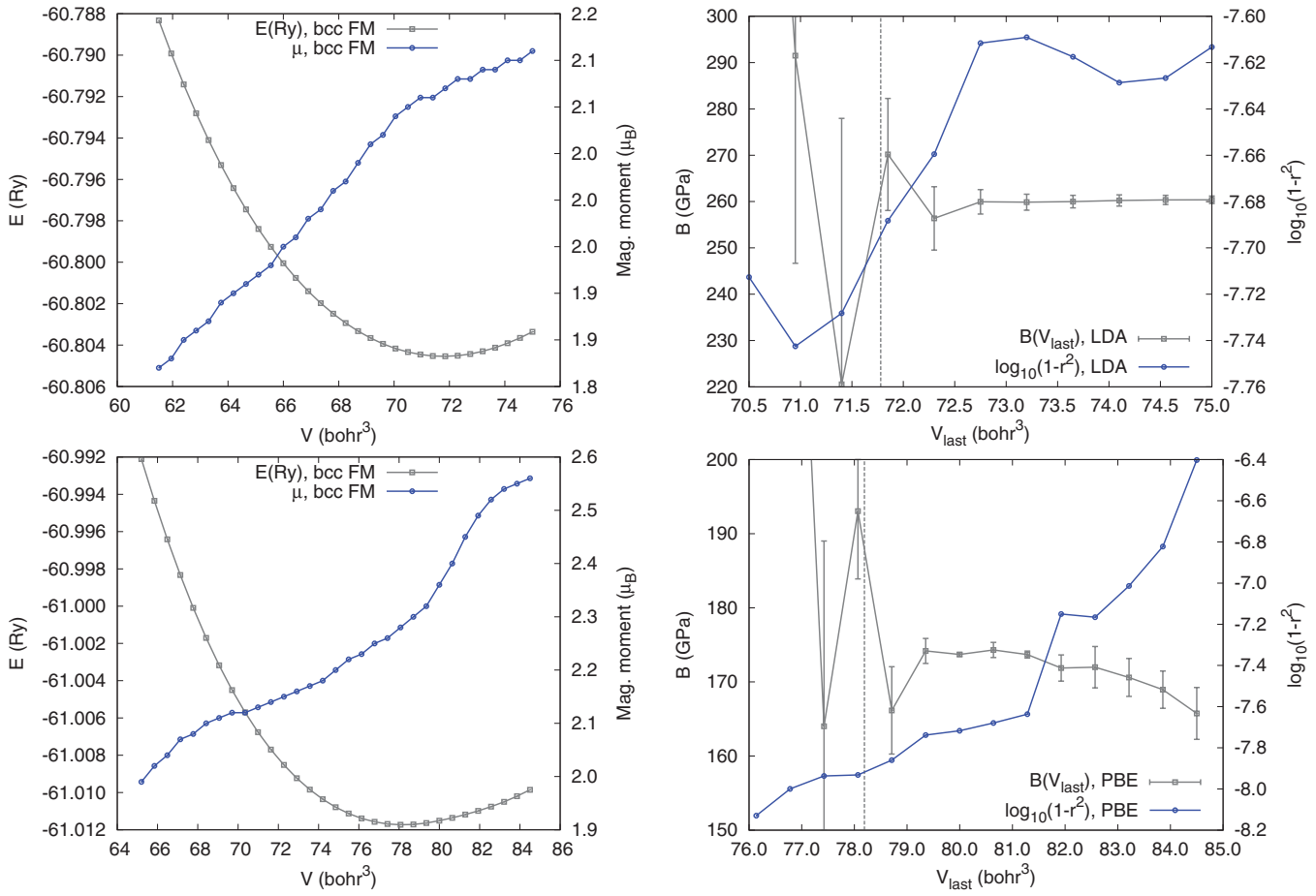

FIG. 8. (Color online) The left-pane graphs depict the calculated static energies and magnetic moments of ferromagnet. The right pane shows the evolution of the bulk modulus with respect to the last point in the volume grid used in the fit, and the associated error bars. The upper plots correspond to LDA and the lower to PBE.

Cold smearing[84] was applied, with smearing parameter equal to 0.01 Ry. The calculated energy ordering at $p = 0$ reproduces results in the literature (see Ref. 85 and references therein). In the calculation of EOS that follows, we use only ferromagnetic bcc and nonmagnetic hcp phases, in accord with experimental results.

The application of the EECs requires a very accurate description of the static energy curve. Achieving this in α-Fe is troublesome because of the magnetic transition at volumes slightly higher than the equilibrium volume. This effect was recently studied by Zhang *et al.* (Ref. 86): the magnetic transition induces a subtle change in the behavior of $E(V)$ that affects the fitted equation of state, which justifies the spread of reported bulk modulus values in the literature.

The problem can be dealt with the strain polynomial averaging technique.[24,25] Figure 8 shows the calculated energies and magnetic moments. The PBE results clearly show the aforementioned magnetic transition on expansion, while the same feature is not present in LDA in the volume range studied. The impact of the transition can be seen in the right pane, where the calculated bulk modulus (and its error bars) are shown against the last volume of the grid used for the fit. Irrespective of the functional, if too few points around the energy minimum are included, the bulk modulus shows that wide variations and error bars are very large, which is consistent with the poor behavior of high-order strain polynomials on extrapolation. The B_0 error bars decrease steadily when considering more points in LDA, where there is no magnetic anomaly, and the phase has "predictable" physical behavior. In PBE, the bulk modulus is affected by including in the fit the volumes where the magnetic transition is taking place, although on a much smaller scale than in the literature.[86] The change in physical behavior of the phase is readily detected by an increase in the size of the error bars. In comparison, the r^2 coefficient of the fit fails to identify the problematic volumes, being monotonically closer to 1 as more points are removed from the end of the grid.

To overcome this situation, we have removed the volumes higher than those of the stable fit zone, and extended the $E(V)$ grid by extrapolation using a low-order strain polynomial.

To avoid the computation of phonon frequencies, we use the Debye-Grüneisen thermal model,[30,32] where the phonon DOS is approximated by (atomic units)

$$g(\omega) = \begin{cases} \frac{9n\omega^2}{\omega_D^3} & \text{if } \omega < \omega_D, \\ 0 & \text{if } \omega \geqslant \omega_D, \end{cases} \tag{37}$$

$$\Theta_D = \frac{1}{k_B}(6\pi^2 V^{1/2} n)^{1/3} f(\sigma)\sqrt{\frac{B_{sta}}{M}}, \tag{38}$$

$$f(\sigma) = \left\{3\left[2\left(\frac{2(1+\sigma)}{3(1-2\sigma)}\right)^{3/2} + \left(\frac{(1+\sigma)}{3(1-\sigma)}\right)^{3/2}\right]^{-1}\right\}^{1/3}, \tag{39}$$

where k_B is the Boltzmann constant, σ the Poisson ratio, M the molecular mass, n the number of atoms per cell, and Θ_D the Debye temperature, directly related to the Debye frequency ω_D. The Poisson ratio of Fe is taken to be 0.3679 (Ref. 87) for the bcc phase and the Cauchy solid value (0.25) for the hcp phase. This thermal model can be applied without information apart from the $E(V)$ curve and possibly the Poisson ratio.

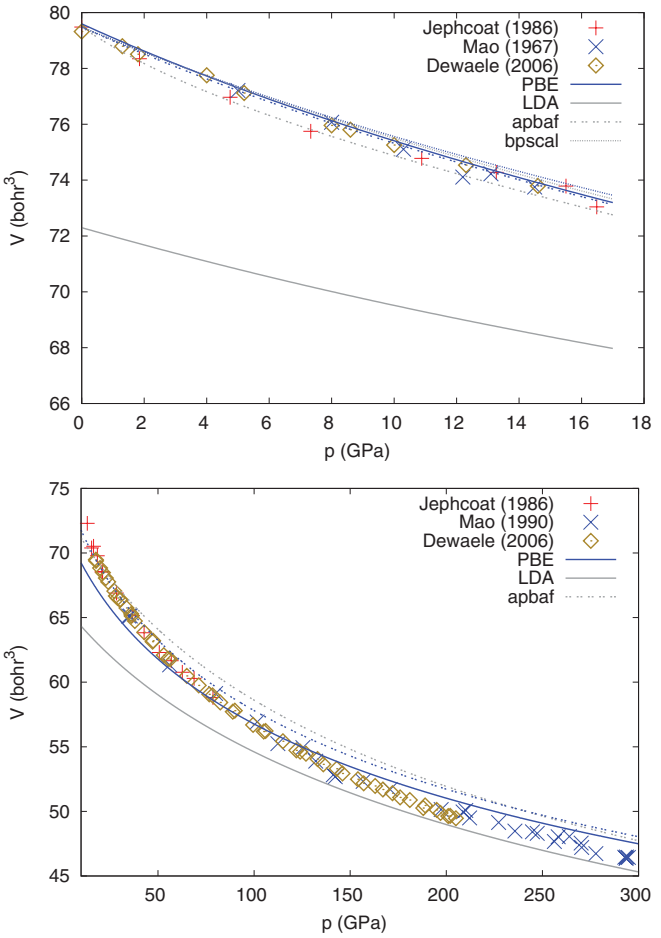

FIG. 9. (Color online) Calculated and experimental equation of state of α-Fe (up) and ε-Fe (down). The experimental data correspond to Refs. 88–91.

A consequence of the appearance of B_{sta} in Eq. (38) is that, contrary to what happens when using the exact phonon DOS, the EECs affect the thermal model. This problem is easily solved by applying the EEC correction iteratively until convergence. In practice, convergence is achieved in less than six iterations.

The ε-Fe phase has only been observed at high pressure. In order to apply the EECs, it is necessary to generalize Eqs. (6)–(19) to the case where experimental volumes and bulk moduli are provided at arbitrary external pressures (p_{ext}) and temperatures (T_{ext}). It is easily found that the general form of these equations still applies in this case, but replacing the thermal pressure with $p_{th} - p_{ext}$ and the room temperature with T_{ext}.

The calculated equations of state of α-Fe and ε-Fe are shown in Fig. 9. In the α phase, we used the APBAF ($V^0_{expt} = 79.4818$ bohr^3) and the BPSCAL ($B^0_{expt} = 169$ GPa[86]) corrections. Iron is a particular system in that LDA and PBE results do not bracket the correct equilibrium volume.[7] In Fig. 9, we can see that the PBE equation of state is barely affected by the correction because the uncorrected value is close to experimental data. However, the poor LDA equation of state is effectively corrected by APBAF and BPSCAL. As it happened with aluminum, diamond, and MgO, the BPSCAL

correction brings LDA, PBE, and experimental results into close agreement.

This agreement with experiment is slightly worse in the case of ε-Fe. Lacking the bulk modulus data, we use only the APBAF correction at $p = 17.7$ GPa ($V^0_{\text{expt}} = 69.4809$ bohr^3).[91] The EOS agree with experimental values close to the correction point and up to around 100 GPa in the case of PBE, but systematically overestimate the volume past this zone.

The phase transition in uncorrected PBE is 24.7 GPa, and upon correction with BPSCAL, the corrected value is 42.8 GPa. The uncorrected and especially the corrected result compare poorly with experiment [the transition takes place between 13.8 and 16.2 GPa (Ref. 81)]. Again, this effect can be ascribed to the problems in the treatment of the hcp phase, the limitations of the thermal model, or the importance of an adequate treatment of magnetism.[7,92]

Several reasons can account for the deviations in ε-Fe EOS: (i) the Debye-Grüneisen model employed is too simple to reproduce the phase behavior over a very wide pressure range; (ii) the experimental error in the volume used in the correction may affect the behavior of the curve; and (iii) the error caused by the exchange-correlation functional can not be traced back solely to static energy. The latter has been studied by Hatt *et al.*[7] and is likely to apply to other magnetic materials as well, where LDA and GGA yield very different magnetic and vibrational properties. The exchange-correlation functional errors in these systems are, therefore, not limited to volumetric effects, and the EECs correct only part of the problem.

VII. CONCLUSIONS

In this paper, we have shown how, under current practice, DFT calculation of thermodynamic properties and equations of state in the quasiharmonic approximation fail to reliably predict equations of state and thermodynamic properties. To solve this problem, caused by the systematic error trends displayed by exchange-correlation functionals, we propose modifying the calculated static energy by using empirical energy corrections (EECs).

The EECs described modify the static energy, but not the volume-dependent vibrational properties obtained as derivatives of the static energy. The corrections make use of one (PSHIFT, APBAF) or two (BPSCAL) experimental data. In the version presented in this paper, these data are the ambient conditions volume and, optionally, the isothermal bulk modulus. By proper application of the temperature model, the experimental data are exactly reproduced by the corrected calculation, modulo uncertainties caused by the fitting procedures.

The comparison of the predicted equations of state and thermodynamic properties with experimental results show an improvement that corrects the systematic deviations of LDA and PBE functionals. In the particular case of PBE combined with BPSCAL corrections (and, depending on the objective property, the APBAF EEC), all properties examined are predicted within experimental accuracy for wide ranges of pressure and temperature, i.e., from very low to very high values of p and T. As a simple application of this methodology, we propose a very accurate p-V-T equation of state for MgO, diamond, and fcc aluminum using a Mie-Grüneisen-Debye expression.

The analysis of thermodynamic properties related to higher derivatives of the energy show that the validity range of the quasiharmonic approximation is functional dependent: the temperature upper bound is consistently higher for uncorrected LDA than for PBE, and even higher for any corrected PBE. This result casts a doubt on the usability of LDA for geophysical studies, as high-temperature uncorrected LDA results can be subject to large errors or fortuitous cancellations between the well-known overbinding and the unphysical softening caused by the lack of anharmonic corrections. In such a case, a positive comparison to experiment in a pressure-temperature region where this cancellation happens can lead to a disastrous extrapolation to other conditions, where no experimental data are available and it is necessary to have a reliable prediction.

Furthermore, having a correct equation of state is fundamental when comparing with the experimental results of properties that depend critically on volume such as the phonon density of states or the frequencies at the Γ point. The improvement extends to other properties (electronic, magnetic) as well, provided they are correctly treated at DFT level.

We have examined the correction of the Gibbs free energy $G(p,T)$, a key component of the calculation of phase diagrams. We conclude that the correction is important when different phases of the solid are compared, and that it is driven by the $p\Delta V$ term at high pressures and by the ΔF_{vib} term at high temperatures, both depending critically on the correctness of the underlying equation of state.

Finally, we have shown how a simplified correction scheme is possible using an approximate thermal model such as the Debye-Grüneisen scheme. The systematic deviations in the equations of state are partially corrected, but the accuracy achieved is less than in the extraordinary results provided by the full QHA calculation. The extreme computational cheapness of the approximate models might justify considering its results as a provisional first test.

ACKNOWLEDGMENTS

We thank the Spanish Ministerio de Ciencia e Innovación (MICINN), Grant No. CTQ2009-08376, and the Malta/Consolider initiative Grant No. CSD2007-00045. A.O.R. is indebted to the Spanish Ministerio de Educación y Ciencia (MEC) for a FPU grant.

*Current address: School of Natural Sciences, University of California, Merced, 5200 North Lake Road, Merced, California 95343, USA; aoterodelaroza@ucmerced.edu

†victor@carbono.quimica.uniovi.es

[1] P. Hohenberg and W. Kohn, Phys. Rev. B **136**, B864 (1964).

[2] W. Kohn and L. J. Sham, Phys. Rev. **140**, 1133 (1965).

[3] M. Born and K. Huang, *Dynamical Theory of Crystal Lattices* (Oxford University Press, New York, 1988).

[4] D. C. Wallace, *Thermodynamics of Crystals* (Dover, New York, 1972).

[5] S. Narasimhan and S. de Gironcoli, Phys. Rev. B **65**, 064302 (2002).
[6] S. Mehta, G. D. Price, and D. Alfè, J. Chem. Phys. **125**, 194507 (2006).
[7] A. J. Hatt, B. C. Melot, and S. Narasimhan, Phys. Rev. B **82**, 134418 (2010).
[8] V. N. Staroverov, G. E. Scuseria, J. Tao, and J. P. Perdew, Phys. Rev. B **69**, 075102 (2004).
[9] G. I. Csonka, J. P. Perdew, A. Ruzsinszky, P. H. T. Philipsen, S. Lebegue, J. Paier, O. A. Vydrov, and J. G. Angyan, Phys. Rev. B **79**, 155107 (2009).
[10] P. Haas, F. Tran, P. Blaha, K. Schwarz, and R. Laskowski, Phys. Rev. B **80**, 195109 (2009).
[11] P. Haas, F. Tran, and P. Blaha, Phys. Rev. B **79**, 085104 (2009).
[12] B. Grabowski, T. Hickel, and J. Neugebauer, Phys. Rev. B **76**, 024309 (2007).
[13] A. van de Walle and G. Ceder, Phys. Rev. B **59**, 14992 (1999).
[14] K. Kunc and K. Syassen, Phys. Rev. B **81**, 134102 (2010).
[15] L. Schimka, J. Harl, and G. Kresse, J. Chem. Phys. **134**, 024116 (2011).
[16] F. Favot and A. Dal Corso, Phys. Rev. B **60**, 11427 (1999).
[17] A. Dal Corso and S. de Gironcoli, Phys. Rev. B **62**, 273 (2000).
[18] A. A. Quong and A. Y. Liu, Phys. Rev. B **56**, 7767 (1997).
[19] A. Zupan, P. Blaha, K. Schwarz, and J. P. Perdew, Phys. Rev. B **58**, 11266 (1998).
[20] J. P. Perdew and K. Schmidt, *Density Functional Theory and Its Application to Materials* (AIP, Melville, NY, 2001).
[21] A. Otero-de-la Roza and V. Luaña, Phys. Rev. B (to be published).
[22] S. Baroni, S. de Gironcoli, A. Dal Corso, and P. Giannozzi, Rev. Mod. Phys. **73**, 515 (2001).
[23] P. Carrier, R. M. Wentzcovitch, and J. Tsuchiya, Phys. Rev. B **76**, 064116 (2007).
[24] A. Otero-de-la Roza and V. Luaña, Comput. Phys. Commun. **182**, 1708 (2011).
[25] A. Otero-de-la Roza and V. Luaña, Comput. Theor. Chem. **975**, 111 (2011).
[26] Z. Q. Wu, R. M. Wentzcovitch, K. Umemoto, B. S. Li, K. Hirose, and J. C. Zheng, J. Geophys. Res. **113**, B06204 (2008).
[27] Z. Q. Wu, R. M. Wentzcovitch, K. Umemoto, B. S. Li, K. Hirose, and J. C. Zheng, J. Geophys. Res. **115**, B05201 (2010).
[28] A. B. Alchagirov, J. P. Perdew, J. C. Boettger, R. C. Albers, and C. Fiolhais, Phys. Rev. B **63**, 224115 (2001).
[29] M. A. Blanco, E. Francisco, and V. Luaña, Comput. Phys. Commun. **158**, 57 (2004).
[30] A. Otero-de-la Roza, V. Luaña, and D. Abbasi, Comput. Phys. Commun. **182**, 2232 (2011).
[31] J. Slater, *Introduction to Chemical Physics* (McGraw-Hill, New York, 1939).
[32] V. L. Moruzzi, J. F. Janak, and K. Schwarz, Phys. Rev. B **37**, 790 (1988).
[33] P. Giannozzi, S. Baroni, N. Bonini, M. Calandra, R. Car, C. Cavazzoni, D. Ceresoli, G. L. Chiarotti, M. Cococcioni, I. Dabo, A. Dal Corso, S. de Gironcoli, S. Fabris, G. Fratesi, R. Gebauer, U. Gerstmann, C. Gougoussis, A. Kokalj, M. Lazzeri, L. Martin-Samos, N. Marzari, F. Mauri, R. Mazzarello, S. Paolini, A. Pasquarello, L. Paulatto, C. Sbraccia, S. Scandolo, G. Sclauzero, A. P. Seitsonen, A. Smogunov, P. Umari, and R. M. Wentzcovitch, J. Phys. Condens. Matter **21**, 395502 (2009) [http://www.quantum-espresso.org].
[34] D. Vanderbilt, Phys. Rev. B **41**, 7892 (1990).
[35] J. P. Perdew and A. Zunger, Phys. Rev. B **23**, 5048 (1981).
[36] J. P. Perdew, K. Burke, and M. Ernzerhof, Phys. Rev. Lett. **77**, 3865 (1996).
[37] B. Li, K. Woody, and J. Kung, J. Geophys. Res. **111**, B11206 (2006).
[38] F. Occelli, P. Loubeyre, and R. LeToullec, Nat. Mater. **2**, 151 (2003).
[39] K. Syassen and W. B. Holzapfel, J. Appl. Phys. **49**, 4427 (1978).
[40] A. Dewaele, P. Loubeyre, and M. Mezouar, Phys. Rev. B **70**, 094112 (2004).
[41] N. W. Ashcroft and N. D. Mermin, *Solid State Physics* (Thomson Learning, London, 1976).
[42] N. D. Mermin, Phys. Rev. **137**, A1441 (1965).
[43] S. Speziale, C. S. Zha, T. S. Duffy, R. J. Hemley, and H. K. Mao, J. Geophys. Res. **106**, 515 (2001).
[44] Y. Tange, Y. Nishihara, and T. Tsuchiya, J. Geophys. Res. **114**, B03208 (2009).
[45] G. Fiquet, D. Andrault, J. P. Itié, P. Gillet, and P. Richet, Phys. Earth Planet. Inter. **95**, 1 (1996).
[46] S. V. Sinogeikin, J. M. Jackson, B. O'Neill, J. W. Palko, and J. D. Bass, Rev. Sci. Instrum. **71**, 201 (2000).
[47] L. S. Dubrovinsky and S. K. Saxena, Phys. Chem. Miner. **24**, 547 (1997).
[48] A. Dewaele, F. Datchi, P. Loubeyre, and M. Mezouar, Phys. Rev. B **77**, 094106 (2008).
[49] R. Reeber and K. Wang, J. Electron. Mater. **25**, 63 (1996).
[50] A. D. Chijioke, W. J. Nellis, and I. F. Silvera, J. Appl. Phys. **98**, 073526 (2005).
[51] Y. Akahama, M. Nishimura, K. Kinoshita, H. Kawamura, and Y. Ohishi, Phys. Rev. Lett. **96**, 045505 (2006).
[52] G. Langelaan and S. Saimoto, Rev. Sci. Instrum. **70**, 3413 (1999).
[53] Y. Wang, Z. K. Liu, L. Q. Chen, L. Burakovsky, and R. Ahuja, J. Appl. Phys. **100**, 023533 (2006).
[54] O. Anderson and K. Zou, J. Phys. Chem. Ref. Data **19**, 69 (1990).
[55] M. Jacobs and R. Schmid-Fetzer, Phys. Chem. Miner. **37**, 1 (2010).
[56] *CRC Handbook of Chemistry and Physics*, edited by D. R. Lide and W. M. Haynes (CRC Press, Boca Raton, FL, 2010).
[57] R. Vogelgesang, A. K. Ramdas, S. Rodriguez, M. Grimsditch, and T. R. Anthony, Phys. Rev. B **54**, 3989 (1996).
[58] C. S. Zha, H. K. Mao, and R. J. Hemley, Proc. Natl. Acad. Sci. USA **97**, 13494 (2000).
[59] E. S. Zouboulis, M. Grimsditch, A. K. Ramdas, and S. Rodriguez, Phys. Rev. B **57**, 2889 (1998).
[60] H. J. McSkimin and P. Andreatch, J. Appl. Phys. **43**, 2944 (1972).
[61] G. N. Kamm and G. A. Alers, J. Appl. Phys. **35**, 327 (1964).
[62] D. Gerlich and E. S. Fisher, J. Phys. Chem. Solids **30**, 1197 (1969).
[63] R. R. Reeber, K. Goessel, and K. Wang, Eur. J. Mineral. **7**, 1039 (1995).
[64] G. A. Slack and S. F. Bartram, J. Appl. Phys. **46**, 89 (1975).
[65] A. C. Victor, J. Chem. Phys. **36**, 1903 (1962).
[66] E. D. Eastman, A. M. Williams, and T. F. Young, J. Am. Chem. Soc. **46**, 1178 (1924).
[67] W. F. Giauque and P. F. Meads, J. Am. Chem. Soc. **63**, 1897 (1941).
[68] D. B. Fraser and A. C. H. Hallett, Can. J. Phys. **43**, 193 (1965).
[69] A. J. Leadbetter, J. Phys. C: Solid State Phys. **1**, 1481 (1968).
[70] D. B. Downie and J. F. Martin, J. Chem. Thermodyn. **12**, 779 (1980).
[71] P. D. Pathak and N. G. Vasavada, J. Phys. C: Solid State Phys. **3**, L44 (1970).

[72]R. M. Nicklow and R. A. Young, Phys. Rev. **129**, 1936 (1963).
[73]*Thermophysical Properties of Matter*, edited by Y. Touloukian (IFI/Plenum, New York, 1970).
[74]R. M. Wentzcovitch, B. B. Karki, M. Cococcioni, and S. de Gironcoli, Phys. Rev. Lett. **92**, 018501 (2004).
[75]R. Stedman, L. Almqvist, and G. Nilsson, Phys. Rev. **162**, 549 (1967).
[76]R. M. Wentzcovitch, Y. G. Yu, and Z. Wu, in *Theoretical and Computational Methods in Mineral Physics: Geophysical Applications*, Reviews in Mineralogy & Geochemistry, edited by R. Wentzcovitch and L. Stixrude (Mineralogical Society of America and Geochemical Society, Washington, DC, 2010), Vol. 71, pp. 59–98.
[77]A. S. Mikhaylushkin, S. I. Simak, L. Dubrovinsky, N. Dubrovinskaia, B. Johansson, and I. A. Abrikosov, Phys. Rev. Lett. **99**, 165505 (2007).
[78]A. B. Belonoshko, P. I. Dorogokupets, B. Johansson, S. K. Saxena, and L. Koči, Phys. Rev. B **78**, 104107 (2008).
[79]S. Tateno, K. Hirose, Y. Ohishi, and Y. Tatsumi, Science **330**, 359 (2010).
[80]T. Ishikawa, T. Tsuchiya, and J. Tsuchiya, Phys. Rev. B **83**, 212101 (2011).
[81]O. Mathon, F. Baudelet, J. P. Itié, A. Polian, M. d'Astuto, J. C. Chervin, and S. Pascarelli, Phys. Rev. Lett. **93**, 255503 (2004).
[82]G. Steinle-Neumann, L. Stixrude, and R. Cohen, Proc. Natl. Acad. Sci. USA **101**, 33 (2004).
[83]H. C. Hsueh, J. Crain, G. Y. Guo, H. Y. Chen, C. C. Lee, K. P. Chang, and H. L. Shih, Phys. Rev. B **66**, 052420 (2002).
[84]N. Marzari, D. Vanderbilt, A. De Vita, and M. C. Payne, Phys. Rev. Lett. **82**, 3296 (1999).
[85]E. G. Moroni, G. Kresse, J. Hafner, and J. Furthmüller, Phys. Rev. B **56**, 15629 (1997).
[86]H. L. Zhang, S. Lu, M. P. J. Punkkinen, Q. M. Hu, B. Johansson, and L. Vitos, Phys. Rev. B **82**, 132409 (2010).
[87]J. J. Adams, D. S. Agosta, R. G. Leisure, and H. Ledbetter, J. Appl. Phys. **100**, 113530 (2006).
[88]H. K. Mao, W. A. Bassett, and T. Takahashi, J. Appl. Phys. **38**, 272 (1967).
[89]A. P. Jephcoat, H. K. Mao, and P. M. Bell, J. Geophys. Res. **91**, 4677 (1986).
[90]H. K. Mao, Y. Wu, L. C. Chen, J. F. Shu, and A. P. Jephcoat, J. Geophys. Res. **95**, 21737 (1990).
[91]A. Dewaele, P. Loubeyre, F. Occelli, M. Mezouar, P. I. Dorogokupets, and M. Torrent, Phys. Rev. Lett. **97**, 215504 (2006).
[92]S. Klotz and M. Braden, Phys. Rev. Lett. **85**, 3209 (2000).